ENERGY LABORATORY

MASSACHUSETTS INSTITUTE
OF TECHNOLOGY

CONTROLLED NUCLEATION AND GROWTH PROCESS FOR LARGE GRAINED POLYCRYSTALLINE SILICON PHOTOVOLTAICS

by

Dr. Stephen C. Danforth
and
Dr. John S. Haggerty

MIT-EL 82-028

ABSTRACT

Research has been conducted to develop a new means of producing large grained polycrystlline thin films for photovoltaic applications. The process is one of growth of controlled crystalline nuclei in an a-Si film. For this process to be practicle, we must develop a-Si films with crystallization behavior such that the rate of spontaneous crystallization (nucleation rate) is essentially zero at temperatures where the growth rates are $> 10^4$ Å/min. Amorphous Si films, deposited on oxidized single crystal substrates by RF sputtering, E-beam evaporation, and CVD, have been examined. The spontaneous crystallization behavior and the rates of nucleation and growth of crystals in the Si films have been evaluated using X-ray diffraction and TEM. The results show that microstructural features and impurities in the RF sputtered films result in very high nucleation rates and extremely low growth rates. The CVD films have high nucleation rates associated with the high deposition temperatures. The growth rates for Si crystallites into a-Si in the CVD films are only a factor of 20 below desired levels.

For process demonstration one requires a deposition process that will produce extremely high purity ($\sim 10^{18}/cm^3$) a-Si films at low deposition temperatures. It remains to be seen if this can be done economically by E-beam or conventional CVD processes.

Table of Contents

Contents

List of Figures

List of Tables

List of Symbols

Symbol	Description
δ	Transformation-boundary thickness
ΔF	Free energy difference per mole for phases on the two sides of the boundary
$(\Delta F_A)_G$	Free energy of activation for migration of the transformation boundary
ΔG_c	Gibbs free energy of a critical nucleus
$\Delta_a g^*$	Activation energy for mass transport across the transformation boundary
h	Planck's Constant
I	Nucleation rate
I_{st}	Steady state nucleation rate
k	Boltzmann's Constant
N	Avagadro's number
R	Ideal gas Constant
T	Temperature
T_s	Substrate temperature during deposition
t	Time
τ	Transient time
V_g	Growth rate
μ	Chemical potential
x	Distance
∂	derivative (mathematical operation)
λ	Wavelength

Acknowledgements

The author wishes to thank Drs. John Haggerty and Steve Danforth whose guidance and support were instrumental in this research. I am also indebted to Prof. Ken Russell for his enthusiastic and instructive counsel in bringing this work to fruition. Finally, I wish to thank the many collegues and members of the support staff whose aid made this work possible. Among these are Joe Hillman, Prof. Hank Smith and Michael Geiss. Mr. Hillman deposited the rf-sputtered film and Prof. Smith and Mr. Geiss provided the CVD film used in this study. I also wish to acknowledge the sponsor of this research, SERI (Solar Energy Research Institute) and DOE (Department of Energy) which provided financial support for this project.

I. Introduction

Traditionally, single crystal silicon photovotaic cells have been used to provide electricity from large solar arrays. However, the cost of these devices has limited their use principly to applications where alternative energy sources were impractical. DOE (Department of Energy) estimates that the lowest possible cost for single crystal solar cells is about $1.00/watt.[1] This is 200 to 400% too high to be cost competitive with other energy sources.* However, this cost might be dramatically reduced if thin amorphous or polycrystalline silicon thin films on inexpensive substrates could be substituted for single crystal silicon substrates in solar cells. This could result in a 5000% reduction in the amount of ultra-high purity silicon required for these cells, greatly reducing the cost.**

The difficulty is that solar cells made with amorphous and fine-grained polycrystalline silicon have lower photovoltaic conversion efficiencies than single crystal devices. The highest efficiency achieved for an amorphous cell is 6.5%[3]† at AM1†† and 9.5% at AM1 for a fine-grained polycrystalline silicon device.[4] The typical efficiency of a single crystal silicon device is 15%[4] at AM1.

---

* These numbers depend on whether peak or average power demand is assumed, on the specific energy source, and on the location of the user.

** assuming that the single crystal device is 0.4 mm thick, that cutting and polishing losses are 59% (Ref. 2) and that the vapor-deposited film is 30 μm thick.

† for a hydrogenated amorphous silicon device.

†† illumination equivalent to that of the sun after passing through 1 mile of atmosphere, or 930 W/m^2 of radiant energy.

These relative efficiencies arise from the low electron mobilities through grain boundaries and in amorphous silicon due to electron trapping by dangling bonds and other defects.

The costs associated with any large photovoltaic installation dictate that a minimum conversion efficiency of 10-12% is required for its economic viability.[5] Hence the existing amorphous and fine-grained polycrystalline silicon technologies are inadequate for this application. An attractive alternative would be to create a thin-film polycrystalline silicon device with grain sizes 10-100 times the film thickness.[4] This would minimize the interaction of grain boundaries with electrons in a photovoltaic cell.

Ghosh[6] calculated that a silicon photovoltaic cell using a 20 μm thick film with a 500 μm grain size could have a 10% efficiency. However, the cost could be substantially lower than for a single crystal device.

In a proposal developed at M.I.T.,[7] such a film would be created by laser-irradiating small spots (< 10 μm diam.) on 1000 μm centers in a 30 μm thick amorphous silicon film, to create crystalline nuclei* which subsequently would grow to impingement on anneal. To do this, conditions** must be created under which nucleation can be controlled. In the proposed process, nucleation in amorphous silicon would be controlled by annealing the laser-irradiated silicon film at a

---

* These can be created by melting a thin surface layer of the amorphous silicon film by nanosecond or longer laser pulses (Ref. 9).

** Recrystallization of silicon to achieve large grains is not economic. The rate of grain boundary migration during recrystallization is about 5.8 μm/day at 1396°C (Ref. 8).

temperature below that for spontaneous crystallization of the as-deposited silicon film.

Examination of annealed amorphous silicon films by X-ray diffraction and by selective etching indicated very small characteristic grain sizes in all crystallized films, independent of laser processing. However, neither of these techniques could provide detailed information about the crystallization kinetics in these films.

Therefore, a transmission electron microscope (TEM) investigation was initiated to determine the nature of the processes constraining large-grain growth in these films. The films investigated were ones believed to be promising as candidate materials for growing large-grain polycrystalline silicon thin films by the above process. Nucleation and growth rates during the crystallization of amorphous silicon were measured using the TEM. The chemistry of these films was also investigated.

II. Background

A simple criterion for selecting an appropriate film deposition method and parameters for this selective nucleation and growth process is to chose a film with the maximum crystallization temperature. The rationale was that we wished to maximize growth rates at the crystalline spots (created with a laser) without having this growth terminated by spontaneous crystallization in the a-Si film. Spontaneous crystallization of a-Si was suppressed by annealing the laser-irradiated films below the crystallization temperature of the as-deposited film. The maximum anneal temperature, and hence, the maximum growth rate at the (laser-created) crystalline spots is determined by the crystallization temperature of the as-deposited film in this process.

X-ray diffraction studies of e-beam evaporated, rf-sputtered and chemical vapor deposited (CVD) films were performed in conjunction with Devaud[10] and King[11]. These results suggested that rf-sputtered amorphous silicon films, deposited with the substrate at T_s=400°C, have the highest crystallization temperature, of the samples studied, (Appendix 1).

Growth of polycrystalline spots created with the laser* in this rf-sputtered film was measured by differential etching (Stirl etch) samples before and after annealing at 709 °C for 10 hours. The crystallization temperature was 724 °C, for a 16 hour anneal. The sample, after anneal and etch is shown in Figure 1. The inferred

---

* An argon laser (λ=532 nm) was used. The pulse length was 114 ms at 2.0 W power and the calculated irradiated spot size was 57 μm.

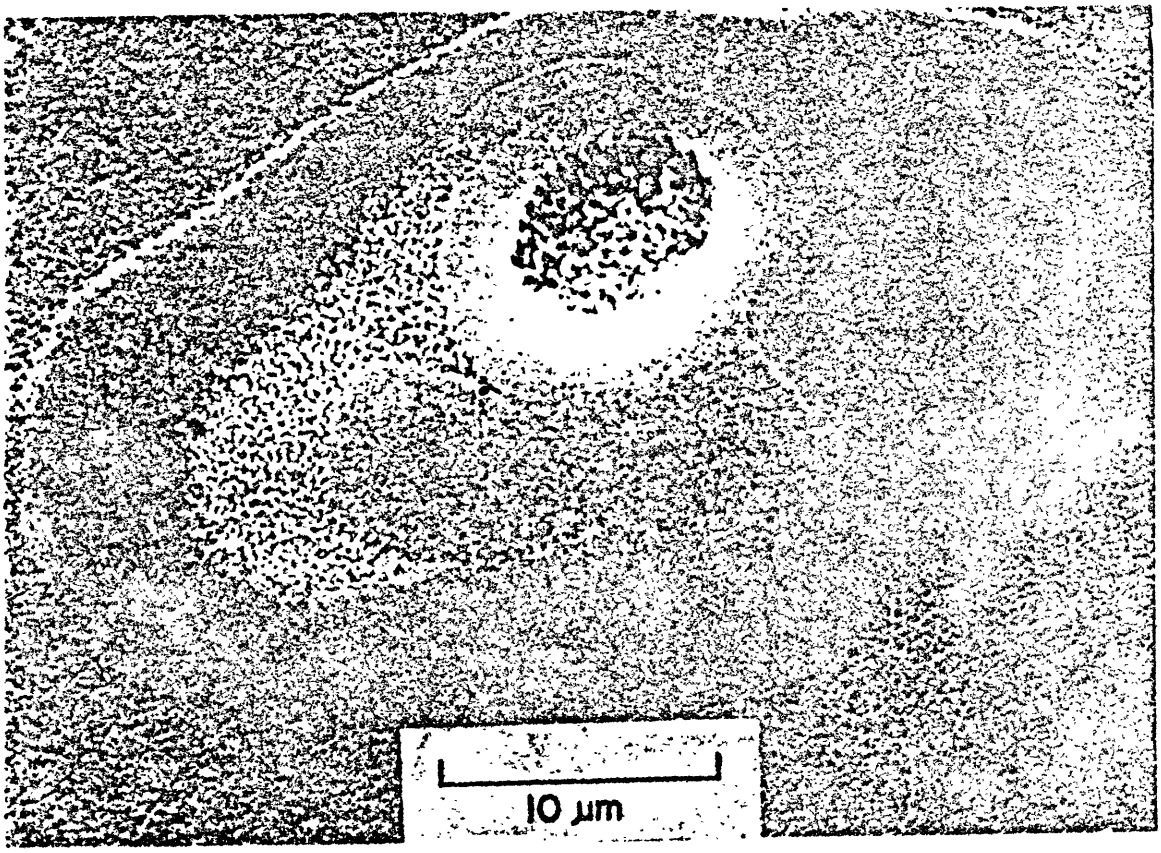

Figure 1: Laser irradiated spot on a rf-sputtered amorphous silicon film after anneal (709°C, 10 hrs) and selective etching.

growth rate of this polycrystalline spot was 2.8×10^{-2} nm/sec at 709 °C. As demonstrated later (see Section III-C-2, Figure 3), this is at least several orders of magnitude lower than growth rates reported by earlier researchers for amorphous silicon deposited by evaporation, or created by ion-implantation.

X-ray line broadening also indicated that the grain sizes in all isothermally annealed amorphous silicon films (1200 nm thick) were no larger than 150 nm for there was no evidence of any spottiness in the diffraction rings.

In the initial stages of the transmission electron microscopy (TEM) investigation of these films, e-beam evaporated, rf-sputtered and CVD deposited amorphous silicon films were considered for further study.

The e-beam evaporated films had two drawbacks relative to project interests. There were severe adhesion problems with these films on the oxidized single crystal silicon substrates. Although this could have been overcome, TEM examination of e-beam evaporated a-Si annealed at 701 °C revealed very irregular crystallites with lenticular or tree-like structures. Therefore, this film did not appear to be promising relative to the requirements of large-grain polycrystalline thin film development.

The CVD film, however, exhibited a well-defined and moderate (100-300 nm) sized grains after annealing at 812°C. Hence this film, and the (OS1-023) rf-sputtered film, (T_s=400°C), were chosen for detailed TEM investigation.

III. Literature Review

A. Steady State Nucleation

The nucleation rate in the crystallization of amorphous silicon (a-Si) depends on many factors. Among these will be the structure of the film at 1-5 nm scale and the nature and distribution of impurities and pores. The later is significant for dangling bonds are active in catalysing both growth, and nucleation-particularly at pore surfaces. Furthermore, amorphous silicon has relatively high densities(10^{20} /cm^3) of internal dangling bonds.[12]

These various effects may be summarized using the expression:*

$$I=N(kT/h)\exp[-(\Delta G_c+\Delta_a g^*)/kT] \qquad (1)$$

for the nucleation rate. $\Delta_a g^*$ is the activation energy for mass transport across the interface and ΔG_c is the Gibbs free energy of a critical nucleus.

The activation energy for nucleation may be determined by fitting the nucleation rate to an Arrhenius type equation. Koster[14] reported an activation energy for nucleation of 469 kJ/mole (4.9eV) for evaporated amorphous silicon (a-Si) deposited at a substrate temperature of T_s=25 °C. This is in very good agreement with that reported by Zellama et al.,[15] 473 kJ/mole (4.9 eV), again for evaporated (T_s=25°C) a-Si. Koster determined this energy using hot-stage TEM, and Zellama by

---

* derived by Turnbull and Fisher (1949) for liquid-solid transformations (Ref. 13)

making electrical conductivity measurements during the crystallization process.

The substrate temperature during deposition seems to affect the activation energy for nucleation. The activation energy for nucleation reported for evaporated a-Si films by Zellama et al.[15] is altered from 473 kJ/mole to 870 kJ/mole as the substrate temperature during deposition is changed from T_s=25°C to T_s=300°C. Zellama et al. attributed this effect to a change in the mode of nucleation, from heterogeneous (surface) nucleation (T_s =25 °C) to bulk, presumably homogeneous nucleation (T_s=300 °C). However, ΔG_c , the energy of forming a critical size cluster, is also expected to vary with the substrate temperature, T_s, with changes in the density and other a-Si film properties.

The nucleation rates for Zellama's evaporated (T_s=300°C) a-Si film are significantly higher than those reported by Koster[14] for evaporated (T_s =25 °C) a-Si, as shown in Figure 2. Zellama did not report nucleation rates for his evaporated films deposited at T_s=25°C.

B. Transient nucleation

In some systems, the time required for the nucleation rate to achieve steady state is a significant fraction of that required for the transformation to reach completion. This is referred to as transient nucleation. Kashchiev[16] has calculated the time-dependent nucleation rate to have the form:

$$I(t)=I_{st}\left[1+2\sum_{m=1}^{\infty}(-1)^m(-m^2t/\tau)\right] \qquad (2)$$

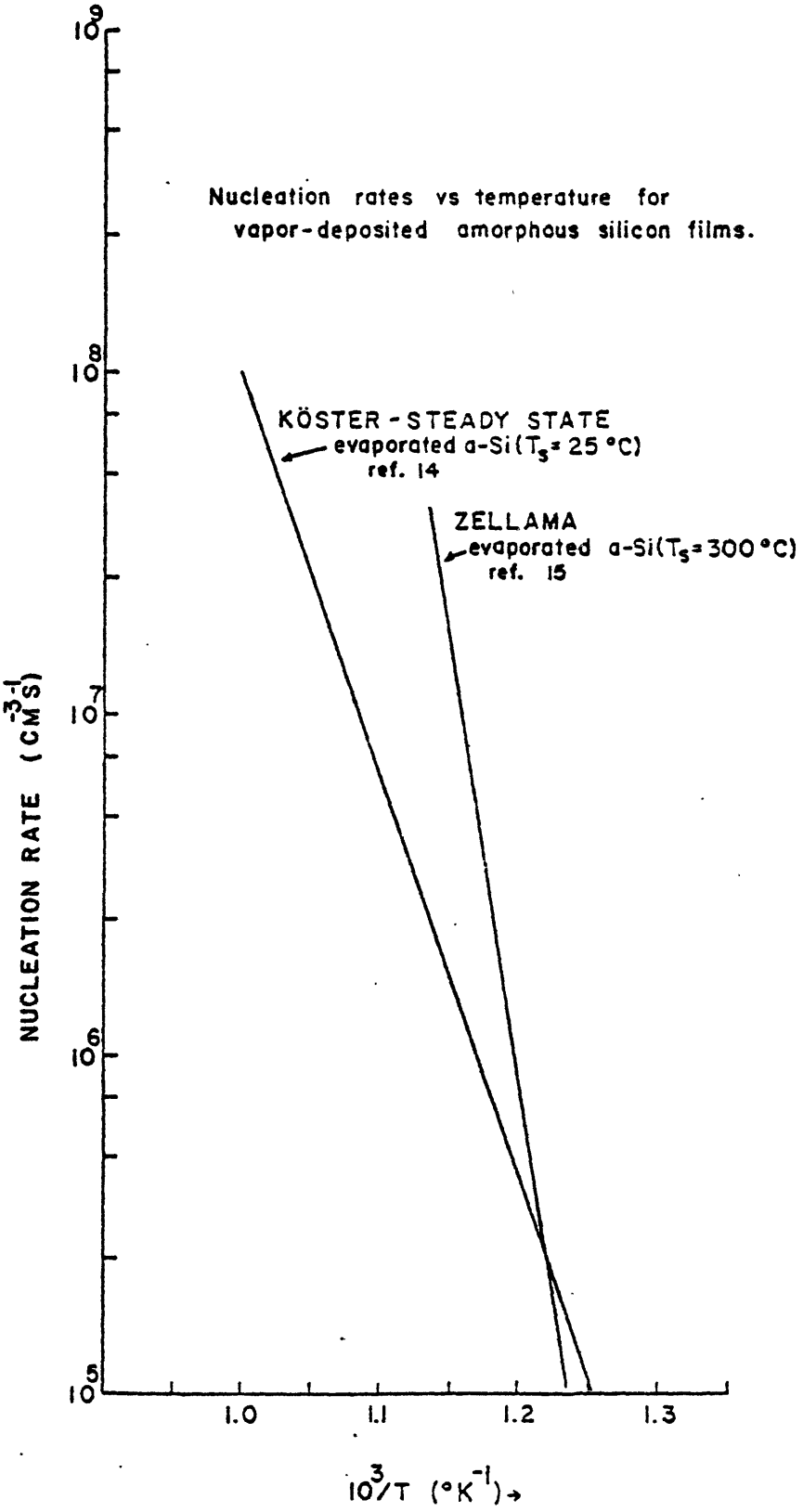

Figure 2: Nucleation rates versus temperature for vapor-deposited a-Si

where τ is the induction or lag time and I_{st} is the steady state nucleation rate.

Koster[14] has reported transient times ranging from 2.5×10^{5} s at 550°C to 2.5×10^{3} s at 650°C, for evaporated (T_s =25 °C) a-Si. These were determined by fitting data from hot-stage TEM experiments to Equation (2).

C. Growth

The character of the growth process, for the crystallization of amorphous silicon, has similarities to surface reconstruction[17,18] in crystalline silicon. This results in anisotropies in growth kinetics which would not be expected for growth of a cubic* crystal in an isotropic medium, as for metals. However, the actual growth rates depend on the density, elastic properties, nature of impurities, and other specifics of the amorphous silicon film.

1. Models

The amorphous/crystalline interface is propagated by breaking bonds in a-Si, thereby allowing silicon atoms to be transferred across the interface to regular lattice-site positions. For growth to occur reliably, this transfer should be to positions where bonding can be established with two atoms which are already in nearest-neighbor positions in the crystalline lattice.[19] This condition is easily met in the <100> direction, as shown in Figure 3 by an examination of the bond angles† and distances required for bonding to crystalline silicon in various growth directions. However, in the <111> direction,

---

* silicon has a diamond cubic structure.
† silicon has tetrahedral coordination.

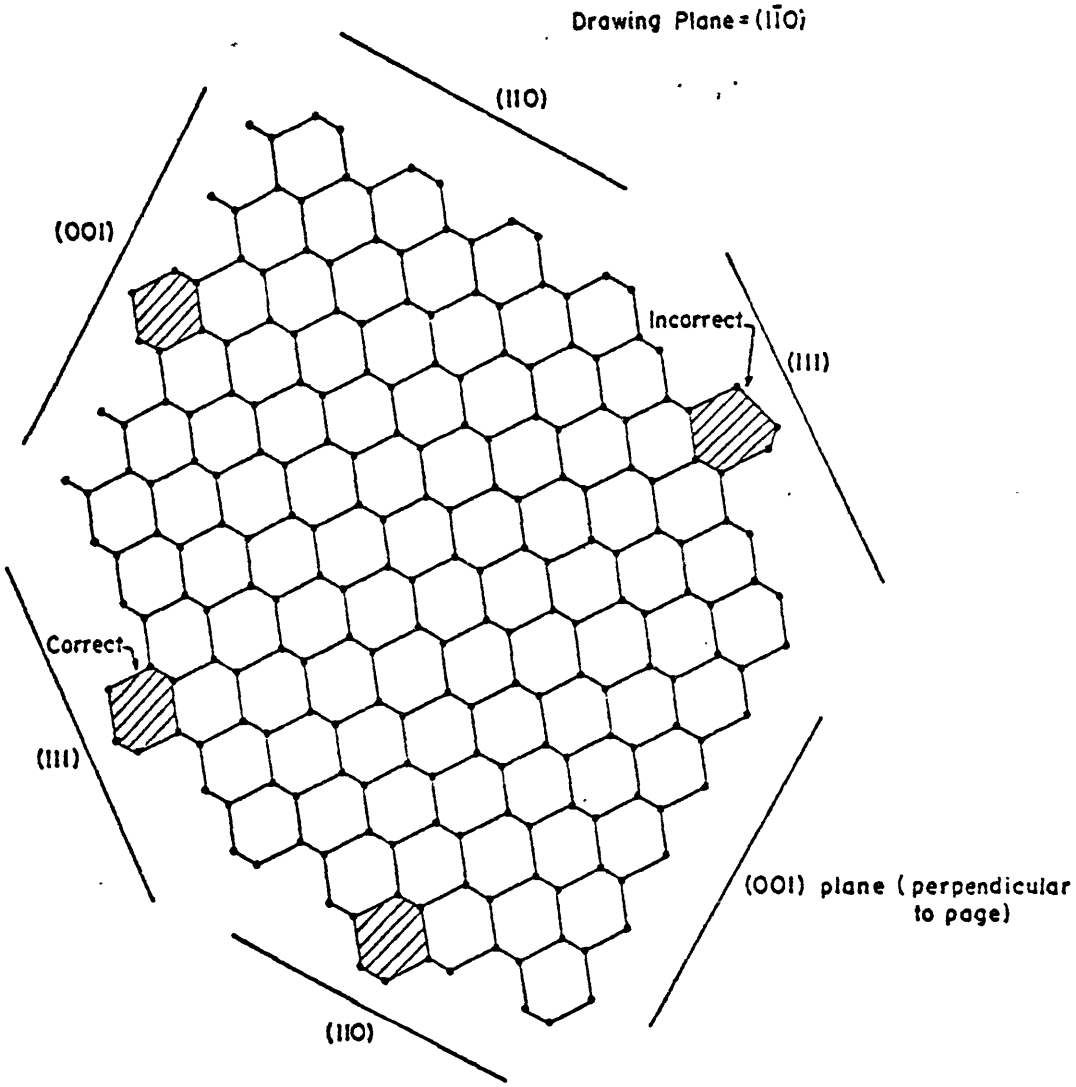

Figure 3, Silicon crystal structure (ref. 19)

alternate planes have atoms with only one bond accessible to atoms crossing the interface, which inhibits the growth process.[19] Drosd speculates that growth along the <111> direction involves nucleation of atomic ledges leading to irregular surfaces and twin formation. Growth in the <111> direction can lead to the formation of a high volume density of twins, reportedly 30-40% at temperatures between 450 and 575°C.[20] The anisotropic character of the growth process results in growth rates which vary by as much as two orders of magnitude for different directions.[20] Growth is fastest in the <100> direction, and slowest in the <111> direction. If the crystallite boundary structure and growth directions are variable, say, due to twin formation during crystallization, anisotropic growth of crystallites could result.[23]

2. Rates and activation energies, pure a-Si.

The kinetics of the regrowth of amorphous silicon created by ion-implantation of single crystal silicon have been investigated by Csepregi[20] and Drosd,[19] but by different methodologies. Whereas Drosd measured growth rates in annealed thin films by TEM, Csepregi used Rutherford (neutron) backscattering to monitor growth rates. As shown in Figure 4, regrowth rates for nearly all orientations and temperatures were higher in Drosd's study than in Csepregi's, by as much as an order of magnitude at 700°C. Furthermore, the activation energies measured also differ significantly. Drosd reported an activation energy of 280 kJ/mole (2.9 eV) for regrowth in the <100>/(010), <110>/(110), <110>/(001), and <111>/(110) orientations (550-650 °C). Growth in the <100>/(010) orientations is growth in the

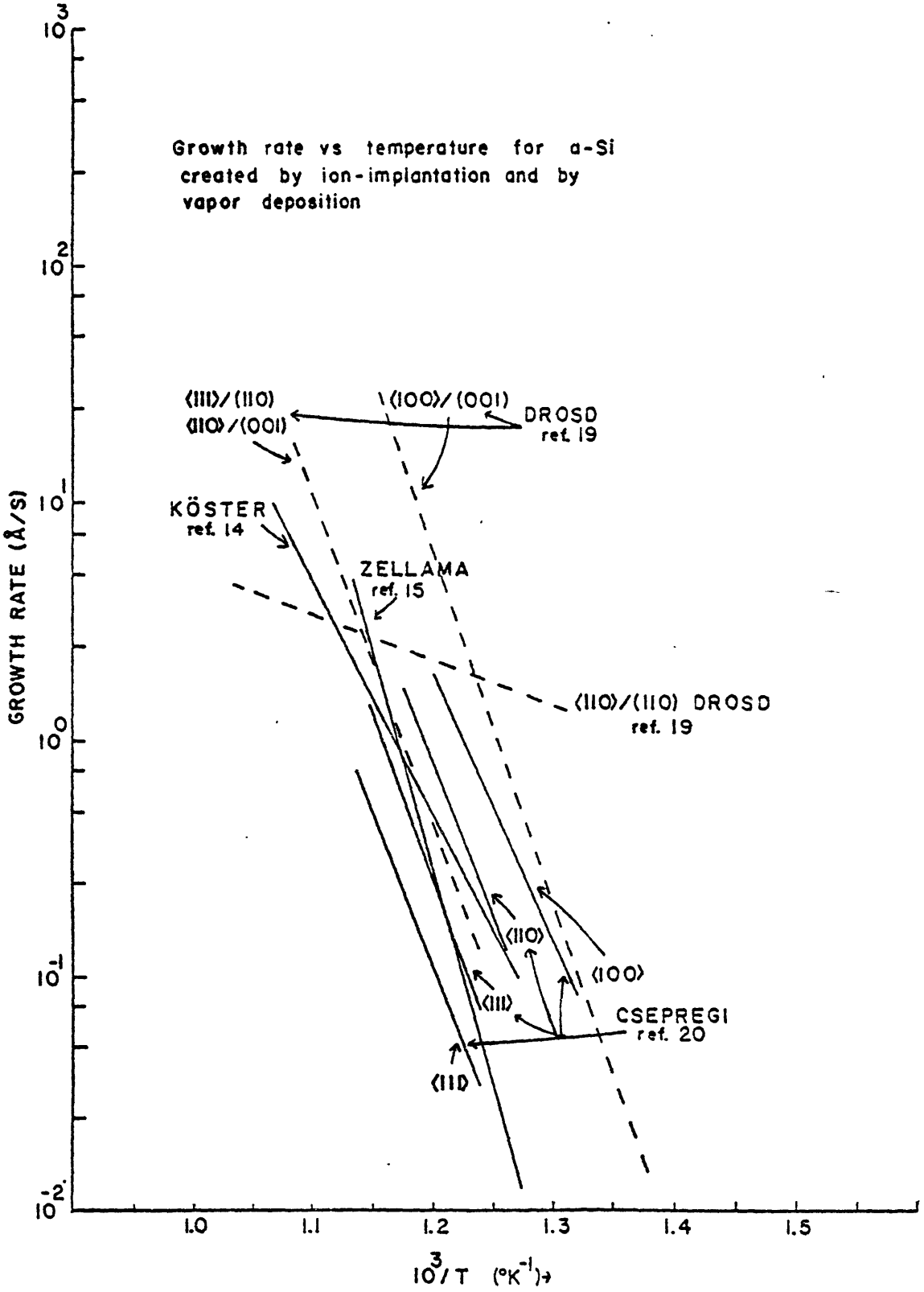

Figure 4: Growth rates versus temperature, pure a-Si

<100> directions where the plane of the silicon substrate from which regrowth initiates is a (010) plane. Csepregi et al.[20], however, cite a somewhat lower activation energy, 232 kJ/mole (2.4 eV) for regrowth in the <100>, <110> and <511> orientations (475-575°C).

Two studies of growth during the crystallization of evaporated amorphous silicon, deposited at T_s=25 °C have been performed. Zellama et al.[15] investigated growth rates by measuring changes in electrical conductivity during crystallization. Koster[14] investigated growth using hot-stage TEM, in which the a-Si foil is annealed in the microscope. The activation energy for growth was reported to be 232 kJ/mole (2.4 eV) by Zellama (560-600°C) and 280 kJ/mole (2.9 eV) by Koster (550- 700 °C). Direct comparision of growth rates is not possible since Zellama did not report this rate for his evaporated a-Si films deposited at T_s=25°C. Zellama did report growth rates for evaporated a-Si deposited at T_s=300°C. However, the activation energy for growth of the T_s=300°C film (473 kJ/mole) is much higher than for these other (T_s=25°C) films.

3. Impurity effects

Impurities in amorphous silicon can either increase or decrease the growth rate during crystallization, as shown in Figure 5. Impurities seem to affect both the activation energy and the driving force (the pre-exponential) for growth, as can be shown using Equation (3).

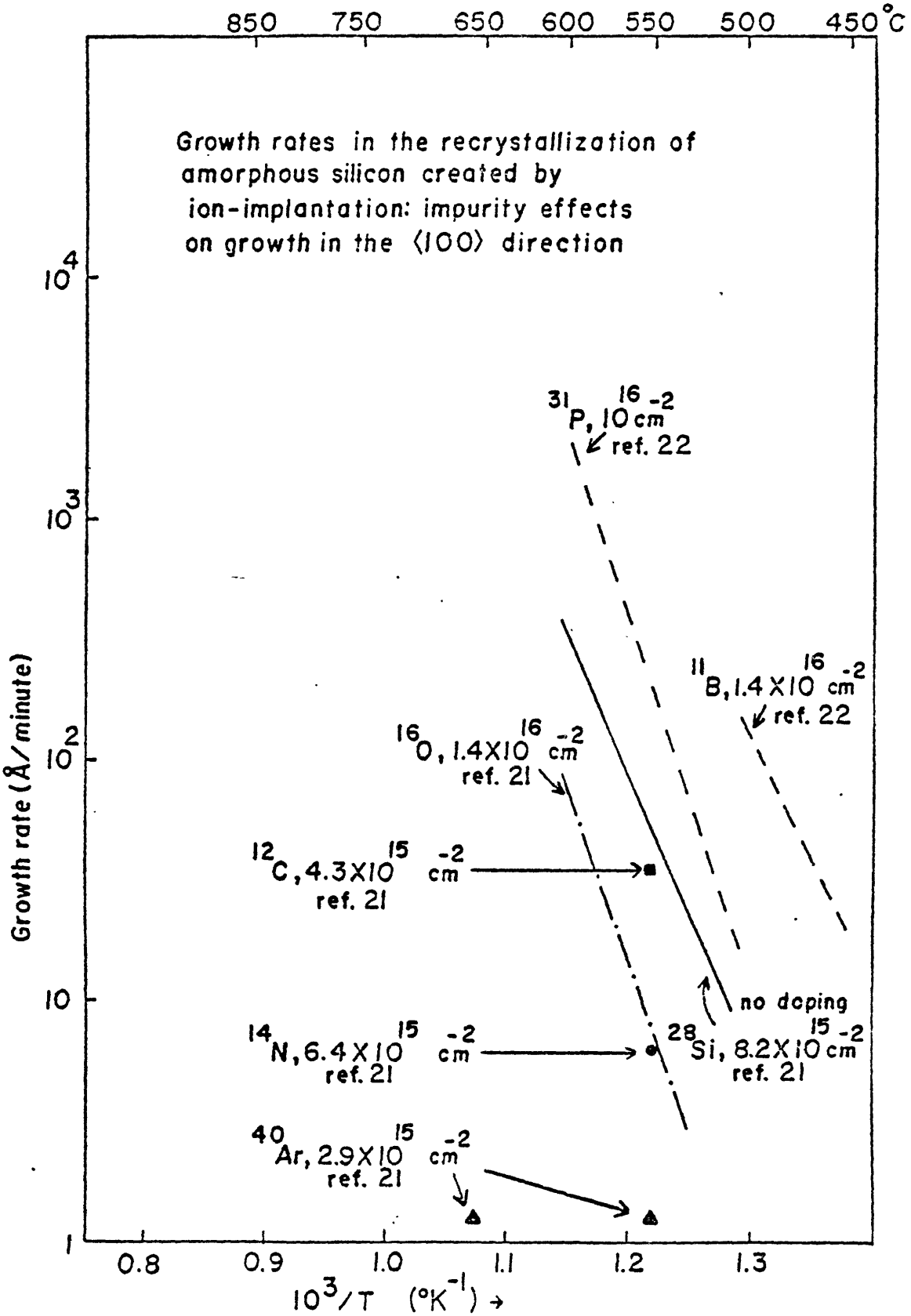

Figure 5: Growth rates versus temperature, impurity effects

4. Effect of a-Si density on growth

The density of amorphous silicon can significantly affect the growth rate. Slight decreases in the density of amorphous silicon from the crystalline value tend to increase the growth rate.[20] Large decreases in the density (8%)* from the crystalline value can reduce the growth rate by an order of magnitude.[24]

5. General expression

In general, the rate of growth during transformation may be described using the expression†:

$$V_g = (kT/h)(\Delta F/RT)\exp[-(\Delta F_A)_G/RT] \qquad (3)$$

where $(\Delta F_A)_G$ is the free energy of activation for transformation boundary migration.

ΔF is the free energy difference per mole for phases on the two sides of the boundary

δ is the boundary thickness

$kT/h \approx 10^{13}\ s^{-1}$ at 700°C

In Turnbull's development,[25] the $\Delta F/RT$ pre-exponential term is associated with the driving force for boundary migration $\frac{\partial \mu}{\partial x} = \frac{-\Delta F}{N\delta}$ where N is Avagadros number. At higher driving forces, this relation is expressed more precisely as

$$V_g = (kT/h)\exp[-(\Delta F_A)_G/RT][1-\exp(\Delta F/RT)]$$

which has been applied to growth in the crystallization of a-Si by Zellama et al.[15]

---

* characteristic of evaporated a-Si films.

† used by Turnbull (Ref. 25) to describe the rate of grain growth in the recrystallization of metals.

IV. Description of Work

A transmission electron microscope (TEM) study of the kinetics of crystallization of amorphous silicon was conducted. The nucleation and growth rates, and their time dependencies were determined. Efforts were made to correlate them to the chemistry and microstructure of the as-deposited films.

The two films principly investigated were deposited by rf-sputtering and chemical vapor deposition (CVD), and were amorphous as determined by electron diffraction. The deposition conditions are specified in Table 1. The CVD film was deposited at Lincoln Labs (M.I.T.) through the efforts of M. Geiss (Lincoln Lab) and Prof. H. Smith (M.I.T.).

These samples were isothermally annealed for various lengths of time (Table 2) and the resulting films examined by TEM. The annealing temperatures were approximately the crystallization temperatures determined by X-ray diffraction (Appendix 1), for a 16 hour anneal.

In a more extensive project the activation energies for nucleation and growth would have been determined. However, a considerable amount of supplimentary data is required to properly interpret these activation energies. Since neither the activation energies or this other data was nessesary to immediate project concerns, measurement of these energies was not actively pursued.

Table 1: Deposition parameters

Rf-sputtered (OS1-023): Polycrystalline Si target

Ultimate Vacuum: 3×10^{-6} Torr

Argon Plasma Pressure: 8.5 mTorr

Accelerating Potential: 1210 V

Substrate Temperature: 400°C

Film Thickness: 1.2 μm

Deposition Rate: 13.3 nm/min

CVD (Chemical Vapor Deposition):

90cc/min 5% SiH_4 in Argon

90cc/min N_2

Total Pressure: 760 Torr (1 atm)

Reactor Temperature: 610°C

Film Thickness: 1 μm

Deposition Rate: 20nm/min

Table 2: Annealing times and temperatures

Rr-sputtered (OS1-023): 724°C for 3.5, 5, 7, 9, and 15 hours

CVD : 551°C for 3, 5, 7, 16, and 23 hours

812°C for 16 hours

A. Experimental Apparatus and Procedure

The experimental procedure was to; obtain a substrate, clean it, deposit amorphous silicon on it, cut or scribe and break it into 1 cm by 1 cm squares, clean if nessesary, perform isothermal anneals of the samples, and prepare TEM specimens. These operations are discussed in terms of their fundamental components; substrates, cleaning procedure, annealing procedure, and TEM-specimen preparation and interpretation.

1. Substrate

Several criterion were developed for selecting an appropriate substrate for this study. An optimum substrate must be:

1) non-crystalline*
2) chemically inert and resistant to diffusion
3) macroscopically, and preferably, microscopically smooth.
4) thermally matched to silicon, i.e. it should have thermal expansion coefficients close to that of silicon.
5) resistant to spalling, or delamination of the silicon film.

Several possible substrate materials which met at least some of these criteria were tested.

Vitreous carbon substrates** were amorphous, had desirable thermal expansion characteristics and were electrically conductive, which would have been desirable for device applications. However, the adhesion of the amorphous silicon was poor, and delamination of small flakes of of silicon occured within a couple of days at room ambient.

---

* to prevent heteroepitaxy or localized strain effects at kinks and cleavage planes on the substrate (Ref. 26).
** Gallard-Schlesinger Chemical Mfg. Corp., Carle Place NY

Fused silica substrates* satisfied the first three criteria. However, a combination of stresses from the crystallization process and from the mismatch of thermal expansion coefficients caused microcracks to propagate through both the deposited layer and into the substrate during anneal.**

Various metals and oxide ceramics (e.g. alumina) were considered and rejected as possible substrate materials due to inadequacies in one or more of the criteria above.

Therefore oxidized single crystal silicon substrates† were employed in this study because they satisfied all of the criteria and were cost effective for research purposes. The oxide layer was 550 nm thick, created by a thermal oxidation process and was amorphous as determined by electron diffraction and dark-field TEM.

2. Cleaning Procedure

The cleaning procedure used for this study consists of degreasing the substrate by successive application of hot trichloroethylene, acetone, methanol and deionized water, as described in Table 3. It has been employed successfully elsewhere for silicon microelectronics research.[28]

---

* Accumet Engineering Corp, Hudson MA
** also reported by Janai et al (Ref. 27)
† Mosfet Micro Labs, Inc., Quakertown PA

Table 3: Substrate cleaning procedure

1) Boil wafer(s) in trichloroethylene for 5 minutes.
2) Ultrasonic clean wafer(s) in hot trichloroethylene for 5 minutes.
3) Heat wafer(s) in acetone to the boiling point.
4) Ultrasonic clean in hot acetone for 5 minutes. Decant.
5) Boil wafer(s) in methanol for 10 minutes. Decant.
6) Ultrasonic clean wafer(s) in distilled, deionized water for 10 minutes.
7) Place wafer(s) on edge, allowing water to run off. A nitrogen gun may be used to assist this process.

3. Deposition Processes

a. rf-sputtered films

A rf (radio frequency) field is applied between two electrodes to accelerate Ar^+ ions toward the silicon target. Silicon is removed and redeposited on the substrate.[29]

A Materials Research Corporation model 8620 rf-sputtering unit was used to deposit the OS1-023 a-Si films used in this study. The substrate-target distance was 5.5 cm. The substrates were heated to 400°C during deposition with an electric heater in the substrate holder (one of the electrodes). A thermally conducting paste insured good thermal contact between the substrate and this heater. The deposition parameters for the rf-sputtered films used in this study are listed in Table 1.

b. Chemical Vapor Deposition

CVD films used in this study were deposited in a low-pressure thermal reactor at Lincoln Labs (M.I.T.), courtesy of Prof. H. Smith and M. Geiss.

The CVD process involves the thermal decomposition of silane gas in the presence of a substrate. Deposition parameters for the CVD films used in this study are listed in Table 1. The reactor used a flowing gas system with argon and nitrogen as carrier gases.

4. Annealing furnace and procedure

A conventional tube furnace was used in all annealing experiments. The sample sat in a high purity alumina boat, in a Vycor (TM) tube which extended through the furnace core. High purity (99.995%, <10 ppm H_2O, <10 ppm O_2) He flowed through the Vycor tube, exiting through

an oil bubbler. An on-off controller regulated temperature via a thermocouple in the furnace. A second thermocouple located next to the sample permitted accurate monitoring of its temperature. The furnace could be brought to temperature without heating the sample by sliding the Vycor tube and sample boat until the later was well outside the furnace core. This was done to minimize the heating times for the sample. The samples remained in the Vycor tube with He flowing until cooled to room temperature at the end of anneal.

5. Transmission Electron Microscopy

Transmission electron microscopy (TEM) involves two related concerns: specimen preparation and image interpretation. Both have inherent difficulties.

a. Specimen preparation

TEM sample preparation consisted of mechanical thinning of the substrate, chemical etching of the substrate (84 ml HNO_3, 28 ml HF, 55 ml acetic acid, 0.125g iodine), and ion-milling to perforation of the deposited layer. The exact procedure used is detailed in Appendix 2. Ion milling was performed at 3-4.5 kV ion accelerating potential and 10-15 degree angle relative to the plane of the plane of the sample. The accelerating potential used increased with the crystallinity of the deposited silicon film.

b. Artifacts

One of the primary difficulties associated with this study was artifacts introduced by the sample preparation technique.

The etching solution used in this study (Appendix 2) had been employed by Drosd[19] for TEM sample preparation of a-Si created by

ion-implantation. However, this etchant left well defined etch pits 5 nm in diameter on the rf-sputtered films. Acid solutions consisting of nitric and hydrofloric acids, and water or acetic acid were found to have slow and non-reproducible etching characteristics if used on small areas or silicon. This was probably associated with the high stability and adhesion of gas bubbles evolved during etching to the sample surface. Another difficulty inherent to chemical etching of a-Si is that the density and chemical reactivity of amorphous silicon changes with the specifics of deposition and heat treatment resulting in highly variable etching behavior. Therefore ion-milling was employed in the final thinning of the samples.

On the basis of an investigation of variables in the ion-milling process, silicon films were milled at 3 kV Ar^+ accelerating potential for a-Si and at 4-5 kV for polycrystalline silicon.

c. Interpretation of TEM results

The effective resolution limit of TEM for detecting second phases in amorphous silicon is about 5 nm[30] in 100-200 nm thick films. This effective resolution limit arises from the nature of inelastic electron scattering processes in a-Si, which result in a non-uniform contrast feature for a-Si in the TEM image. Due to the short range order in a-Si[31] (crystalline coordination to the nearest neighbors), electron scattering processes create regions of electron phase coherency some 1-5 nm in diameter.[32-34] These appear as alternating light and dark or "salt and pepper" contrast features in the TEM image which

have no unique structural interpretation. Transmission electron microscopy was conducted on a Phillips EM300 microscope.*

Other complications arose in interpreting the TEM images of specific samples.

In the OS1-023 (T_s =400 °C) rf-sputtered films, crystallite boundaries could not be reliably resolved from other features in bright-field TEM. Therefore, dark-field TEM was employed in analysing these specimens. In the dark-field technique some, but not all diffracting grains are imaged. These imaged grains will appear bright in the dark-field image. Their intensity will depend on how strongly they diffract (i.e. their orientation relative to the beam), and scattering of electrons as they pass through other grains in the "thin" foil.

The inability to obtain data from bright-field TEM, for the rf-sputtered film, created several difficulties. One of these was possible distortion of the crystallite size distribution by overlaps of diffracting grains resulting in larger apparent crystallite sizes than were the case. The high density of twins in these crystallites, and the associated changes in contrast within the grain made it difficult to judge whether the larger features in dark-field were one crystallite with twins or several overlapping crystallites. Since grain sizes were typically 10 nm in a film 150-200 nm thick, there was a significant probability of multiple grains partially overlapping.

---

* the line resolution (for crystalline samples) of the microscope is 0.9 nm.

In some cases this could be observed by tilting the beam during dark-field TEM work.

The dominant difficulty was in developing a correlation between the density of features in dark-field TEM and the actual crystallite density in the film in the absense of reliable bright-field data. This correlation factor depends principly on the statistics of diffraction processes for the grains in the field of view of the microscope and is estimated in Appendix 3 for the (OS1-023) rf-sputtered film.

V. Results and Discussion

The structure and chemistry, and resulting nucleation and growth behavior during crystallization seem to be specific to the method and parameters of deposition of the amorphous silicon. The nucleation rates for rf-sputter (OS1-023) and CVD deposited amorphous silicon films are substantially higher than reported for some evaporated a-Si films. Growth of crystallites in the rf-sputtered film (OS1-023) seems to be slowed or arrested through a combination of pinning mechanisms including impurity and pore drag. The growth rate in the CVD film was somewhat lower than reported for evaporated a-Si and is anisotropic in character.

A. As-deposited silicon films

The as-deposited (OS1-023) rf-sputtered films exhibited coalescense islands which were polyhedral in shape with an average size of 37.1 nm and a standard deviation of 16.5 nm, (see Micrographs, Figures 6-7). Knights et al.[35] have reported a similiar structure, with coalescense islands 16 nm in diameter in plasma-deposited hydrogenated amorphous silicon (a-Si:H). The relative sizes of these islands may be associated with the difference in substrate temperatures during deposition, T_s =230 °C in Knights study and T_s=400°C in our work. Knights et al[35] performed extensive characterization of their a-Si:H film and concluded that the region between coalescense islands is a low density a-Si structure, not an interconnected pore structure. This, and the high mechanical stability of the very thin sections of the rf-sputtered films used in TEM suggest that the regions between coalescense islands in our films are also a low-density a-Si structure.

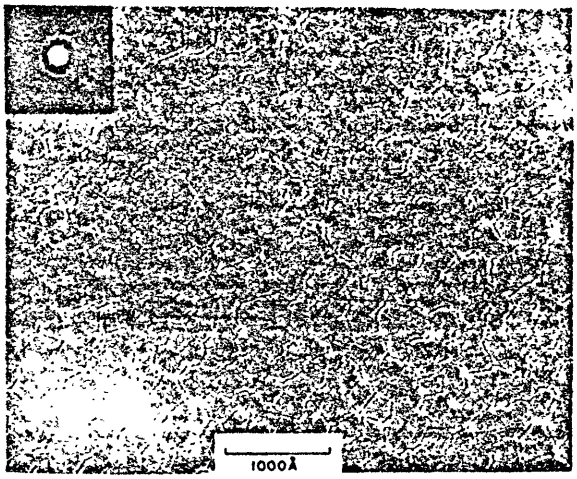

a. Bright-field photo, rf-sputtered (T_s=400°C), as-deposited

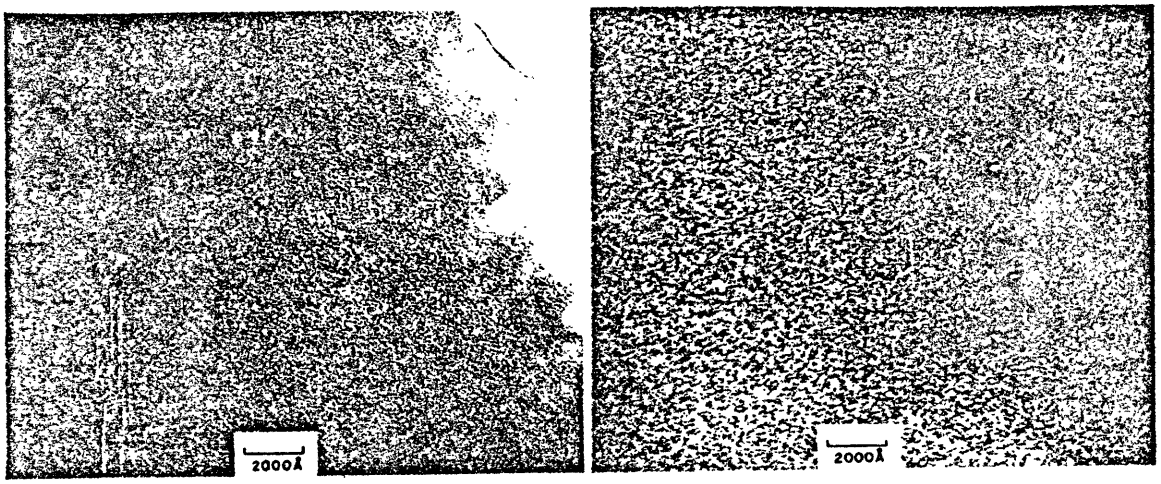

b. Bright (left) and dark (right) field photos of rf-sputtered a-Si after 3.5 hours anneal at 724°C

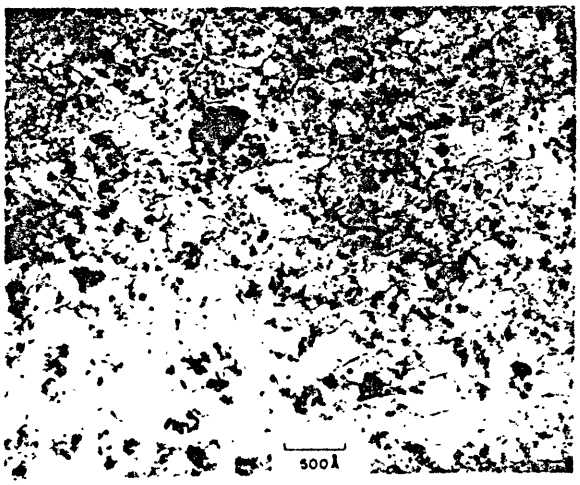

c. Bright-field photo, rf-sputtered a-Si after 7 hour anneal at 724°C

Figure 6: TEM micrographs, rf-sputtered a-Si

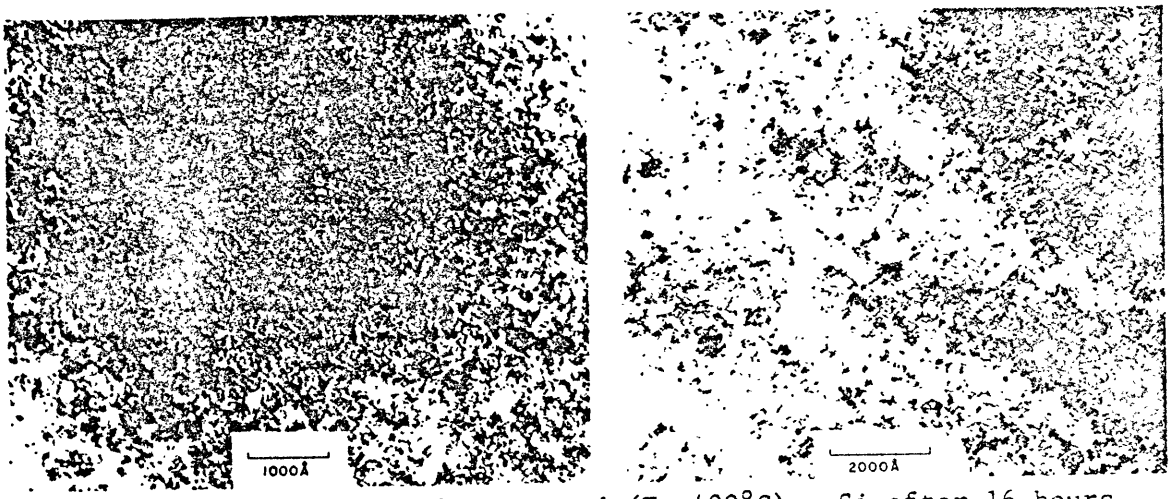

a. Bright-field photos, rf-sputtered (T_s=400°C) a-Si after 16 hours anneal (left) and after 15 hours anneal(right) at 724°C

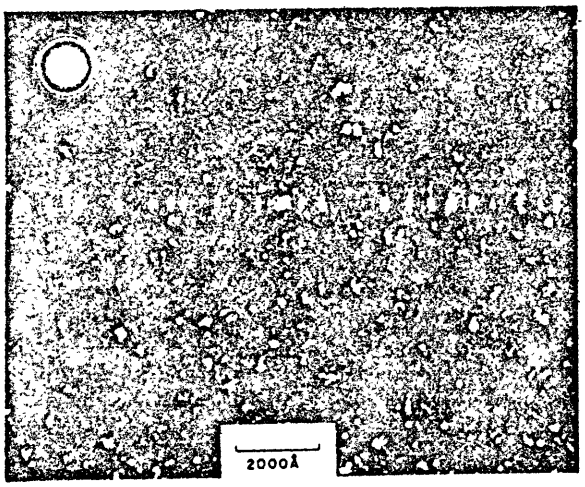

b. Dark-field photos of rf-sputtered (T_s=400°C) after 15 hours anneal at 724°C

Figure 7: TEM micrographs, rf-sputtered a-Si

In contrast, the CVD deposited silicon film of this study exhibited no distinct structure.

Electron diffraction and dark-field TEM results indicated that both of these as-deposited films were amorphous.

B. Determination of crystallinity

Although electron diffraction may be one of the best methods of determining the crystallinity of the samples, it seems that the silicon film can have significant crystallinity before it becomes apparent by this technique. Electron diffraction patterns for CVD deposited silicon indicate an amorphous structure despite the obvious presence of crystallites in both bright and dark-field TEM for CVD films annealed at 551°C for 5 hours, (see Micrographs, Figures 8-9). A similiar difficulty is apparent with X-ray diffraction. X-ray diffraction indicated that (OS1-023) rf-sputtered silicon is amorphous unless annealed at 724 °C or higher temperatures for 16 hours. However, dark-field TEM indicates the presence of some crystallites in this film after only 3.5 hours of anneal at 724°C.

The sensitivity of either of these diffraction techniques to the presence of crystallinity depends significantly on the size and distribution of these crystallites. One reason is that the nearest neighbor coordination in a-Si is identical to that in the crystalline phase.[31] The second and third nearest-neighbor distances are slighly distorted and have a great deal of dispersion relative to the crystalline pnase.[31,37] Additionally, small crystallites would not necessarily have a distinctive diffraction pattern relative to a-Si

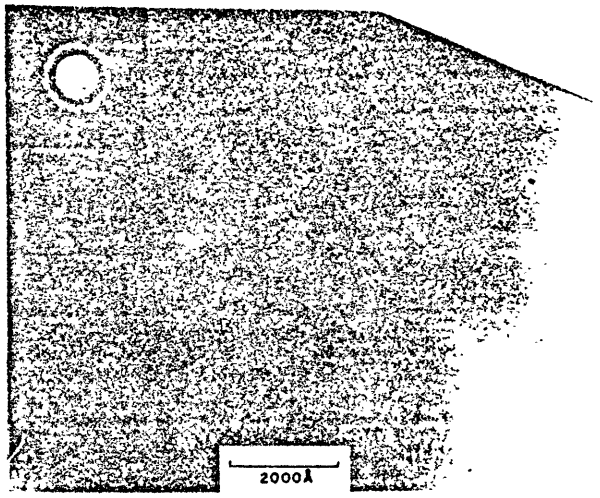

a. Bright-field photo, CVD deposited a-Si after 3 hours anneal at 551°C

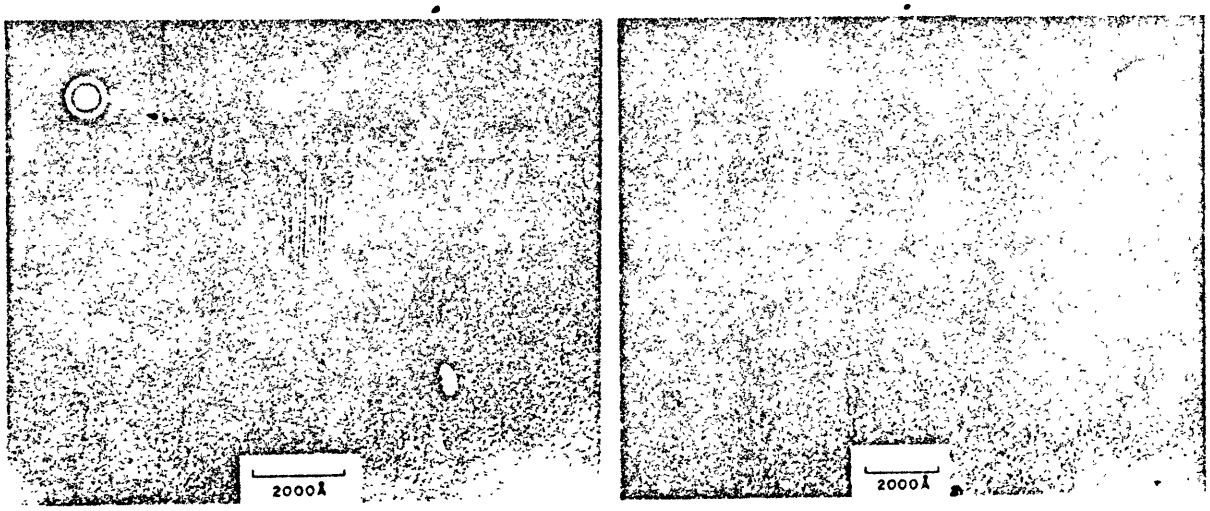

b. Two bright-field photos, CVD deposited a-Si after 5 hours anneal at 551°C

c. Bright (left) and dark (right) field photos of CVD films after 23 hours of anneal at 551°C

Figure 8: TEM micrographs, Chemical Vapor Deposited (CVD) a-Si

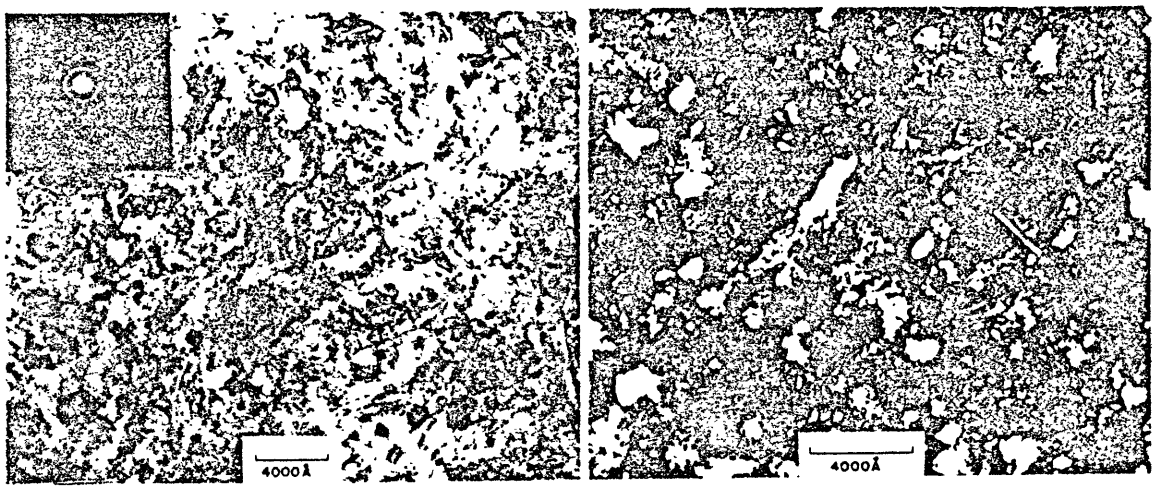

Bright (left) and dark (right) field photos of CVD deposited a-Si after 16 hours anneal at 812°C

Figure 9: TEM micrographs, Chemical Vapor Deposited (CVD) a-Si

due to particle size broadening. Thus, electron diffraction seems to have limited usefulness in detecting small crystallites in a-Si.

Bright-field TEM is considerably more sensitive to the presence of second phases than electron diffraction, but can not be used to uniquely determine whether the second phase is crystalline silicon. Dark-field TEM seems to have a greater sensitivity to the presence of crystallites than electron diffraction or bright-field TEM. The disadvantage of dark-field TEM is that its sensitivity is dependent on the size and distribution of the crystallites. It is statistically reliable only when a large number of crystallites are present in the field of view of the microscope for only those grains diffracting in specific orientations are imaged in dark-field TEM.

C. Rf-sputtered films

1. Nucleation rates

The nucleation rates for our rf-sputtered films were calculated from dark-field data, using the correlation factor calculated in Appendix 3 which was estimated to be a factor of 98 crystallites in the field of view for each one evident in the dark-field TEM images. The number density of features in the dark-field image (see Micrographs, Figures 6-7) was determined assuming a film thickness of 200 nm. The number density was adjusted by the correlation factor and divided by the anneal time to yield an effective nucleation rate.

The steady state nucleation rate for the (OS1-023) rf-sputtered silicon film is 4.1×10^{12} /cm^3 s at 724°C, as determined by linear regression of our nucleation data, (Figure 10). This steady state nucleation rate is four orders of magnitude higher than reported by

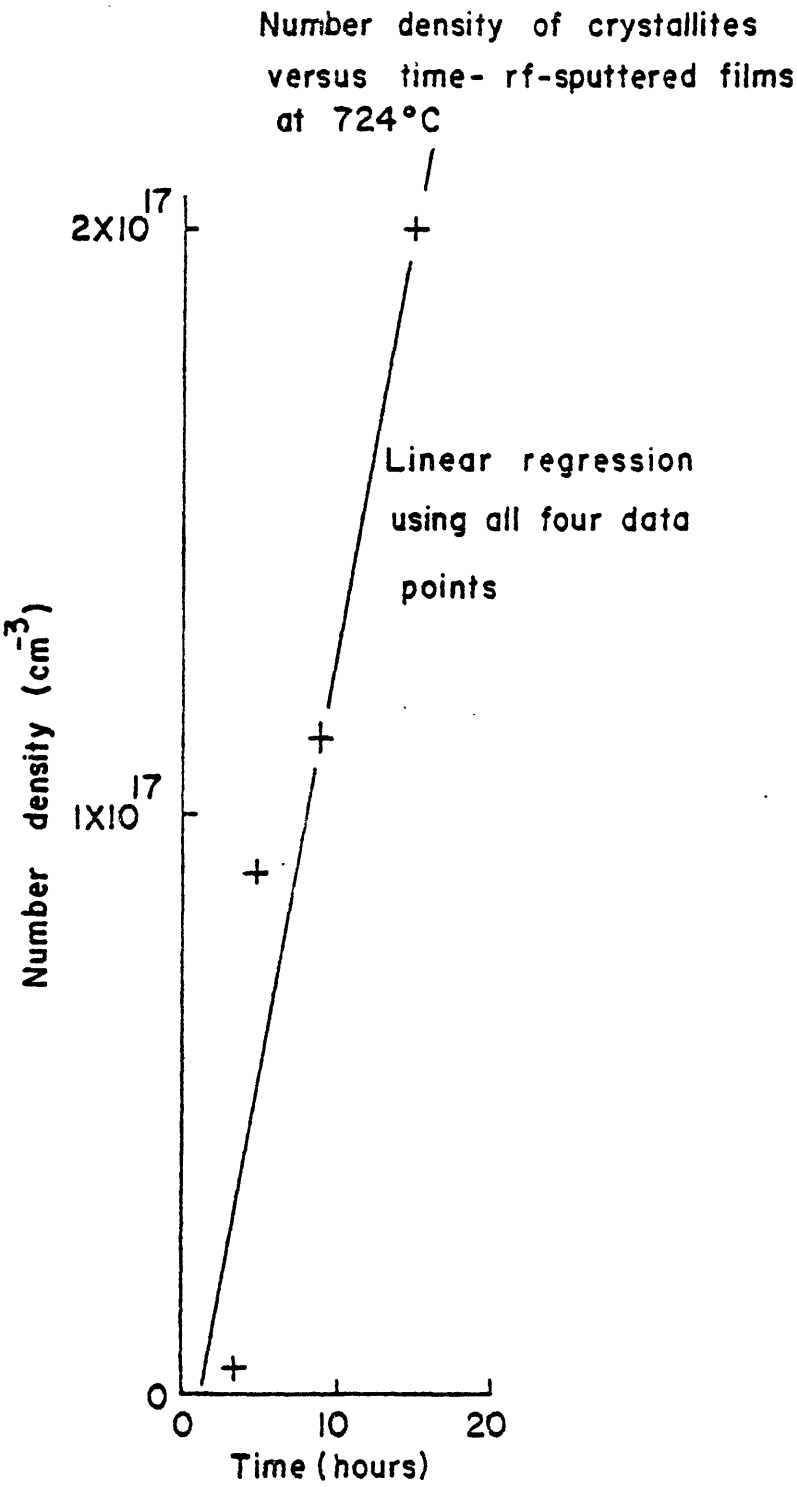

Figure 10: Nucleation behavior with time, rf-sputtered films at 724°C

Koster,[14] at 724°C. However, it is only two orders of magnitude higher than the rate at 724 °C extrapolated from Zellama's data.[15] Both of these were for evaporated a-Si films.

The average nucleation rate over the 3.5 hr anneal is 3.3×10^{11} /cm^3 s (see Table 4), which is an order of magnitude lower than the steady state rate determined by linear regression of our nucleation data (Figure 10). If the difference in these two nucleation rates is associated with a transient effect, a 1.9 hour transient time is calculated using a two term expansion of Equation (2). Koster has reported a transient in nucleation of 41 minutes at 650°C for evaporated (T_s=25°C) a-Si which was calculated using Equation (2). The transient in nucleation for Koster's film should be even smaller at 724°C.[14,16]

2. Growth in rf-sputtered films

Rigorous analysis of the crystallite size distributions to determine the growth rates during the crystallization of rf-sputtered a-Si is non-trivial. The means of the apparent crystallite size distributions depend on both the nucleation and growth rates. The maximum observed sizes give a better indication of the growth rates, but have questionable statistical validity.

Examination of the crystallite size distributions for the rf-sputtered films (Figures 11-12) suggests that no statistical reliablity is gained by using crystallite sizes between the average and maximum sizes in these distributions in growth rate determination since the distributions are not continuous. Finally, the crystallites

Table 4: Nucleation rates, rf-sputtered (0S1-023) a-Si at 724°C

Anneal Time	Average Nucleation rate over the anneal period
3.5 hr	3.3×10^{11} /cm^3 s
5	5.0×10^{12}
9	3.5×10^{12}
15 hr	3.7×10^{12}/cm^{3}s

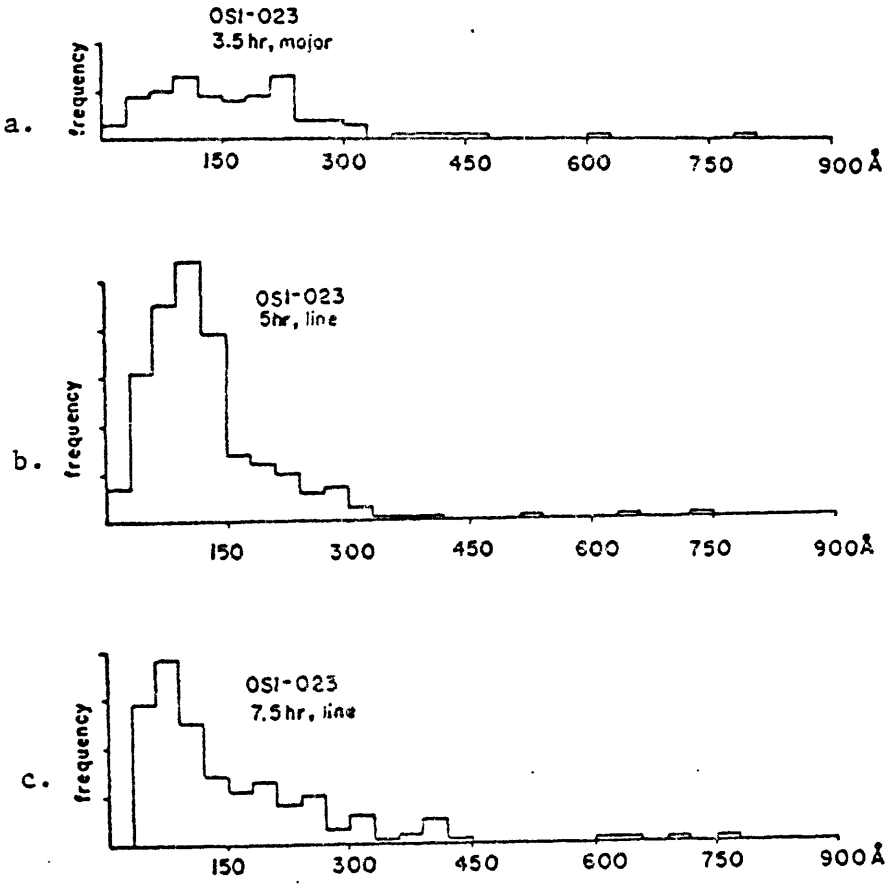

Figure 11: Crystallite size distributions, rf-sputtered films at 724°C
Major-length of major axis measured. This was done on the 3.5 hour sample for the crystallite density in the micrographs was not high enough for reliable line analysis.
Line-length of a random line segment subtending a crystallite measured.

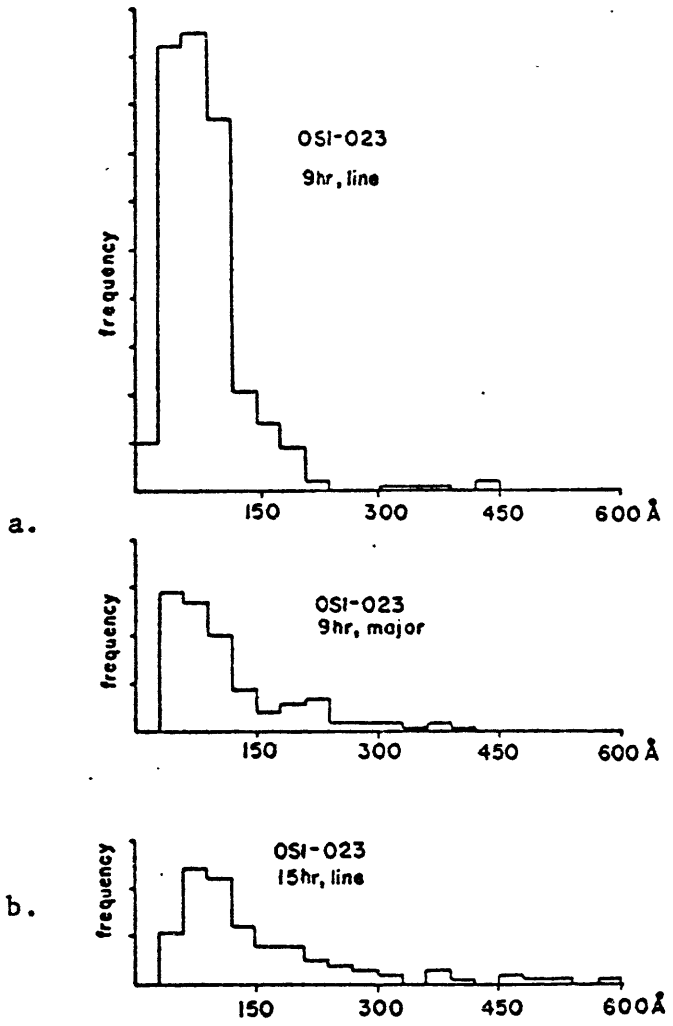

Figure 12: Crystallite size distributions, rf-sputtered films at 724°C
Major-length of major axis was measured
Line- length of a random line segment subtending a crystallite measured. Both major and line analysis performed on the 9 hour sample for comparision, although sample size is different for these two analyses.

in the rf-sputtered film seem to exhibit anisotropic growth, but associated distortions of the size distributions are relatively small. However, some conclusions about the approximate growth rate and time dependencies are possible.

The initial growth rate calculated using the maximum observed crystallite size is 6.4×10^{-3} nm/sec at 724°C for the rf-sputtered film. This growth rate decreases to zero during anneals longer than 3.5 hours at 724°C. The initial growth rate calculated using the mean crystallite size is a factor of 4.6 lower than that calculated using the maximum observed crystallite size. These growth rates are considerably smaller than the growth rates reported for evaporated a-Si at 724°C by Koster,[14] 4.5 nm/sec, or by Zellama,[15] 10 nm/sec.

The growth rate, as measured using the mean crystallite size, slows down over a 5 hour anneal, approaching zero during anneals longer than 7.5 hours, as shown in Figure 13. Furthermore, the maximum observed crystallite size remains approximately constant over anneals longer than 3.5 hours at 724 °C. There are, however, some shifts in the size distribution for it becomes less symetrical with time. The nucleation rate is relatively constant (over anneal times longer than 3.5 hours), suggesting that the growth rate may decrease with increasing volume fraction transformed. The impingement of crystallites should not have significantly affected growth rates for this film becomes crystalline by X-ray diffraction only after 16 hours of anneal at 724 °C. Integration of the steady state nucleation rate over time, combined with an estimate of the volume occupied by each crystallite (assumed size=10 nm) yields a calculated volume percent

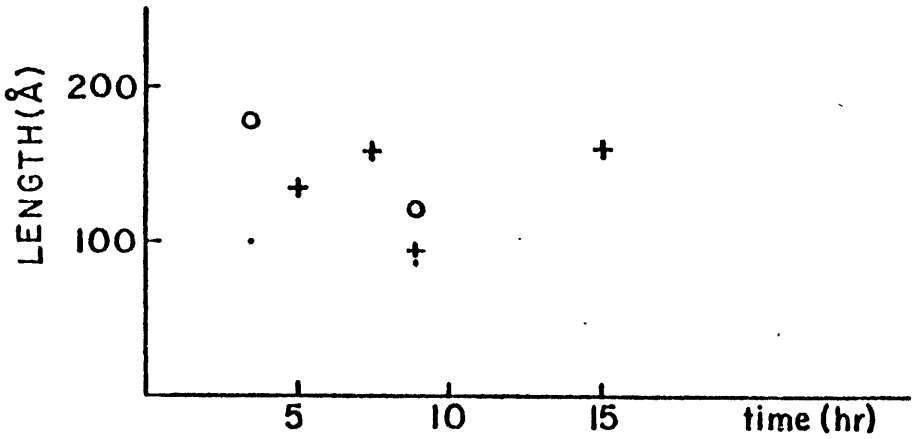

Figure 13: mean sizes vs time rf-sputtered (OSI-023) film annealed at 724 °C

o major axis
· minor axis
+ line-average length of a line segment

Line analysis could not be used reliably on micrographs for the 3.5 hour anneal. Both line(length of a line subtending a crystallite) and point (measurement of major and minor axes) analysis was performed on the 9 hour sample to determine their relationship.

crystallized of 11% after 7.5 hours of anneal at 724 °C, which increases to 23% after 16 hours anneal at 724 °C. Thus, crystallite growth is slowed or arrested in the initial stages of the transformation process. The crystallite size distributions are highly skewed so that the maxima of these distributions (about 10 nm) are probably more representative of the crystallite size than the average sizes in these distributions (about 15 nm).

Two processes may explain the anomalously slow or arrested growth kinetics, pinning of crystallite boundaries by either argon impurities or by pore drag as crystallites impinge on the edges of coalescense islands in the rf-sputtered film.

a. Pinning by argon

Data by other investigators on the regrowth of amorphous silicon created by the implantation of argon into crystalline silicon indicates that argon concentrations in excess of 0.3 at% reduce the regrowth rate about three orders of magnitude (Figure 5), to near zero at 650 °C.[28]

X-ray flourescense performed by I. Kohatsu* indicates that the (OS1-023) rf-sputtered films may contain up to 3.6 at% argon. This estimate is consistent with reports in the literature of 1 to 5 at% argon in rf-sputtered a-Si films.[20,39]

Our SIMS** results indicate that only about 30% of the argon annneals out of the film at 749 °C, over 16 hours. This seems to be comparable to results obtained by Revesz et al.[38] inwhich 30-40% of the

---

* formerly with this project

** performed by Charles Evans&Associates, San Mateo CA

argon (0.5 at% levels) was annealed out of a-Si created by argon and silicon ion-implantation, in 8.3 hours at 630°C. The film thicknesses were 1200 nm and 100 nm, respectively.

Argon is insoluble in crystalline silicon. Hence, as the transformation proceeds, higher concentrations of argon will be present at crystallite boundaries due to rejection of argon from the crystalline phase. As the transformation progresses, this impurity drag effect should become more severe as relatively little of the argon seems to be annealed out of the film.

No evidence was found to indicate the formation of argon bubbles in the rf-sputtered film. The crystallites were typically less than 38 nm in size, hence the formation of argon bubbles small enough to breakaway from the a/c interface,[40] into the crystalline phase would have been a relatively high energy process.[41] Therefore, it seems unlikely that the formation of argon bubbles was significant in reducing the chemical impurity pinning at these boundaries.

b. Pinning at internal boundaries

The boundaries between coalescense islands may also have a significant effect on growth kinetics. Generally, the crystallite sizes were smaller than the average size of these coalescense islands, 37 nm. In all cases in the (OS1-023) rf-sputtered silicon films, the maximum grain size is no larger than about twice the mean coalescense island size (as-deposited), or within two standard deviations of this mean size. The size of the crystallites, therefore, may be limited by the width of these coalescense islands. We were unable to determine if grains actually grew beyond the edges of the coalescense islands,

or whether the presence of crystallites larger than 37 nm was associated with a significant population of coalescense islands with sizes larger than 37 nm. If some grains do grow beyond the edges of these coalescense islands, either of two processes may occur. The first is that pores accumulate at the crystallite boundary, slowing but not arresting growth. The second is that the crystallite doesn't really grow past the coalescense island, but instead nucleates another grain, with an orientation close to that of the original grain, to the other side of the boundary between coalescense islands. With either of these processes, the kinetics of growth past the boundaries are expected to be slow relative to crystallite growth which occurs exclusively within one of these islands.

D. Chemical Vapor Deposited (CVD) films

1. Nucleation

The steady state nucleation rate is 1.8×10^{9} /cm^{3}s at 551°C for the CVD film, as determined from a linear regression of the data. Some variation in this rate is observed both in Table 5 and Figure 14. Even so, this agrees well with the observation of approximately constant nucleation rates for CVD films at 650°C made by Janai et al.[27] This nucleation rate is about four orders of magnitude higher than those measured by Koster[14] or Zellama[15] at 551 °C. The nucleation rates are inferred from bright-field TEM measurements of the number density of crystallites assuming a foil thickness of 200 nm, divided by the anneal time.

Two plausible explainations for this relatively high nucleation rate exist: 1) that deposition by CVD, or by rf-sputtering at

Table 5: Nucleation rates, CVD a-Si at 551°C

Anneal (i)	Time (t_i)	Nucleation rate number over t_i	over $t_i - t_{i-1}$
1	3 hr	3.9×10^9 /cm^{3}s	3.9×10^9 /cm^{3}s
2	5	4.1×10^9	4.4×10^9
3	7	5.5×10^9	9.1×10^9
4	16	1.2×10^9	1.4×10^9
5	23 hr	2.8×10^9 /cm^{3}s	6.3×10^9 /cm^{3}s

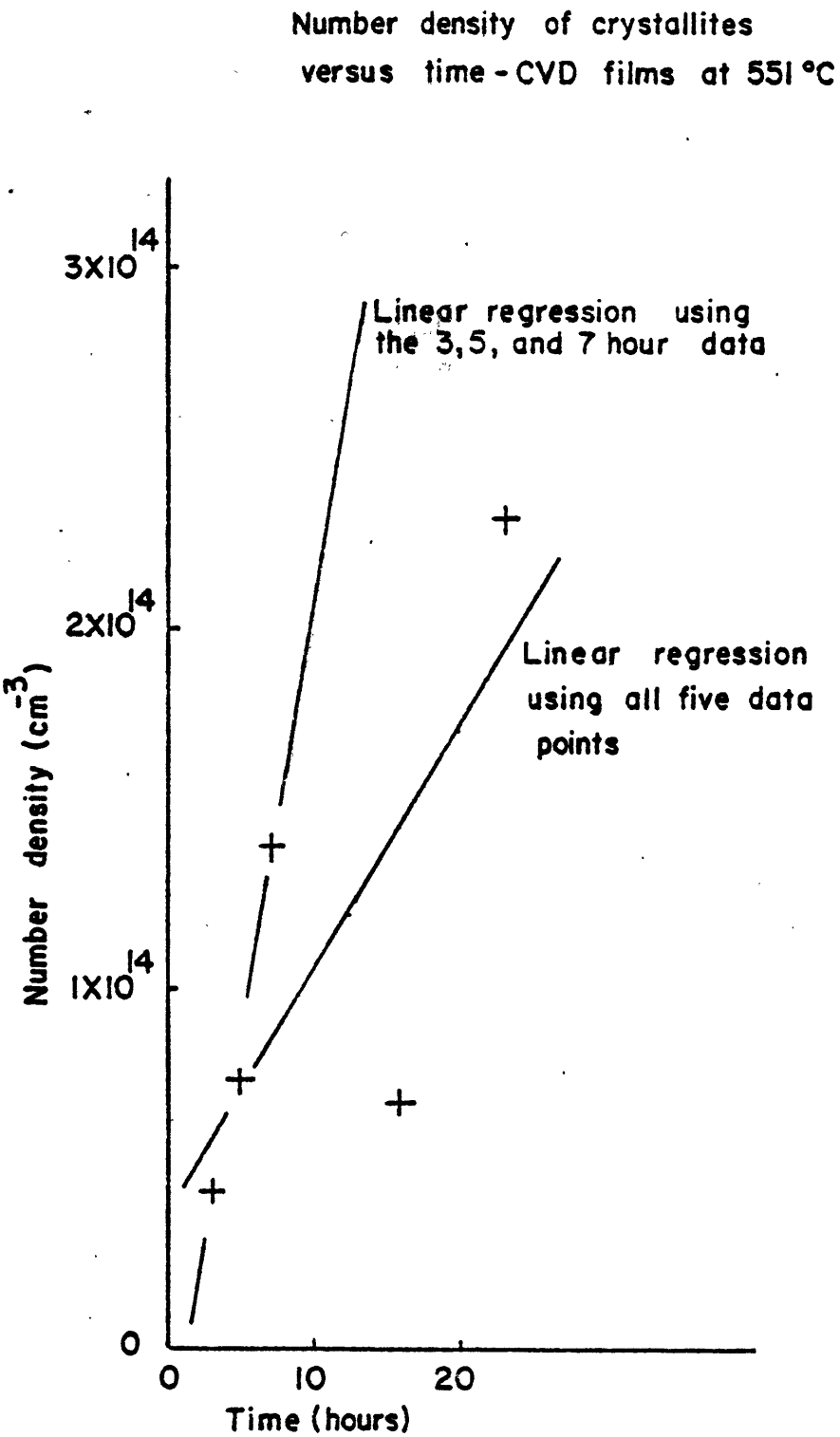

Figure 14: Nucleation behavior with time for CVD films at 551°C

T_s=400 °C alters the cluster size distribution in a-Si resulting in a greater number of crystalline clusters at or near the critical size than is typical for evaporated a-Si, due to differences in the effective deposition temperatures and 2) that heterogeneities in the a-Si film exist at less than 5 nm scale which are active in nucleation but not apparent by TEM. If the later were true, there should be a significant tendency toward preferential nucleation at the edges of coalescense islands in the rf-sputtered film. Nucleation, however, appears to be uniform in these films.

If the nucleation rates for our rf-sputtered and CVD films are compared with the rates reported by Koster[14] and Zellama[15] for evaporated a-Si films, a possible correlation of the deposition temperature and the nucleation rate emerges. The nucleation rate for the rf-sputtered (T_s=400°C) film is over four orders of magnitude higher than for Koster's evaporated a-Si (T_s=25°C) film, but only two orders of magnitude higher than for Zellama's evaporated a-Si (T_s= 300 °C) film, at 724 °C. The nucleation rate for the CVD film (T_s= 610 °C) is four orders of magnitude higher than those measured for either of these evaporated (T_s=25 °C or T_s=300°C) films at 551°C. One possible explaination of these relative rates is that the nucleation rate tends to increase with increasing effective deposition temperature.

The transient in nucleation rate in the CVD (T_s =610 °C) films is neglible at 551°C. The average nucleation rate over the first three hours is close to the steady state value, (Table 5), and the nucleation data, if extrapolated to zero time, indicates no transient

in nucleation-within experimental uncertainty. Koster reported a transient in nucleation of 69 hours at 550°C for evaporated (T_s=25°C) a-Si.[14] A smaller transient would be expected in a CVD film than in an evaporated film for the higher effective deposition temperature of the CVD process should result in a (sub-critical crystalline) cluster size distribution which is much closer to the steady state distribution at the anneal temperature than would be the case for a-Si films deposited by evaporation.

2. Shape Anisotropy (CVD)

The shapes of crystallites in the CVD film are best described as prolate* ellipsoids with eccentricities which tend to increase with increasing size. This is apparent when the axial ratios (major/minor) are plotted against the major axis, as in Figure 15, and in micrographs of the CVD film after anneal (Figures 8-9). When the axial ratio is plotted against the minor axis (Figure 15) no clear trend is evident. As will be shown in the following section, the growth rate along the minor axis is not constant. Differences in growth behavior along the major and minor axes may partially account for the differences in the relationships between the axial ratio and size, along the the two axes. These differences in the relationships of axial ratio to size may be exagerated for the growth anisotropy appears to be statistically but not functionally related to crystallite size for in some instances crystallites which were 30-50 nm (major axis) in size had axial ratios of 6.5-10, respectively.

---

* prolate ellipsoids are formed by rotating an ellipse about its major axis.

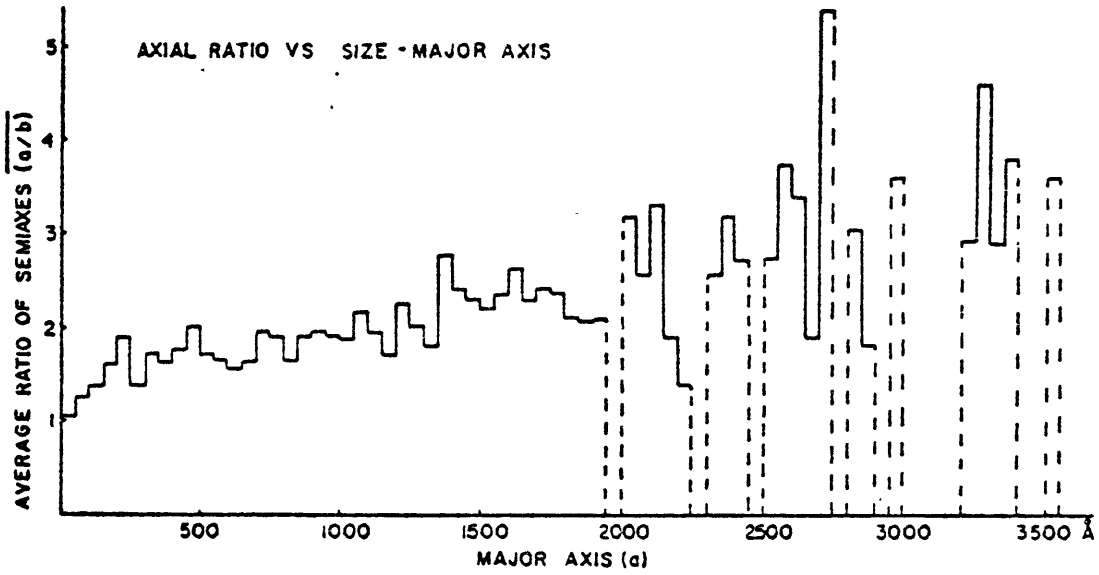

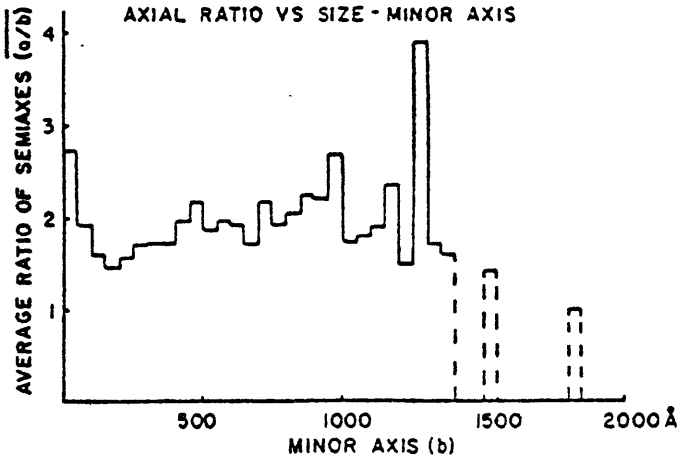

Figure 15: Axial ratio vs size for CVD film at 551°C

Since the eccentricity of the crystallites change, growth data was obtained for both the major (a) and minor (b) axes.

3. Growth in the CVD film

Given the nature of the crystallite size distributions (Figures 16-17), two measures of growth rates in the CVD film may be used, the growth in the mean and in the maximum of this distribution.

As indicated earlier, the mean of the crystallite size distribution tends to be sensitive to the nucleation rate. In the CVD a-Si film, this is manifested in two ways. First, the maximum size in the distribution grows 33 times faster than the size at which the maximum in the distribution occurs, at 551°C. Second, small maxima and minima in the measured nucleation rates for the 7 and 16 hour anneals at 551°C (Table 5, Section V-D-1) seem to correspond to inflection points and maxima in the plots of the mean of the major, and minor axes versus time (Figure 18). These apparent correlations between fluctuations in the nucleation rate and the behavior of the means of the crystallite size distributions are significant, both because of the implied limitation on using the means to calculate growth rates, and because they indicate systematic fluctuations in the nucleation rate.

Another possible measure of growth rates, that calculated from the maximum observed crystallite sizes, seems to yield reasonable and consistent growth rates. The maximum of the major axes is linear in time, and the fit fairly good (Figure 19). This fit implies that the maximum observed crystallite sizes can be used with some confidence in estimating growth rates. However, the maximum of the minor axis is

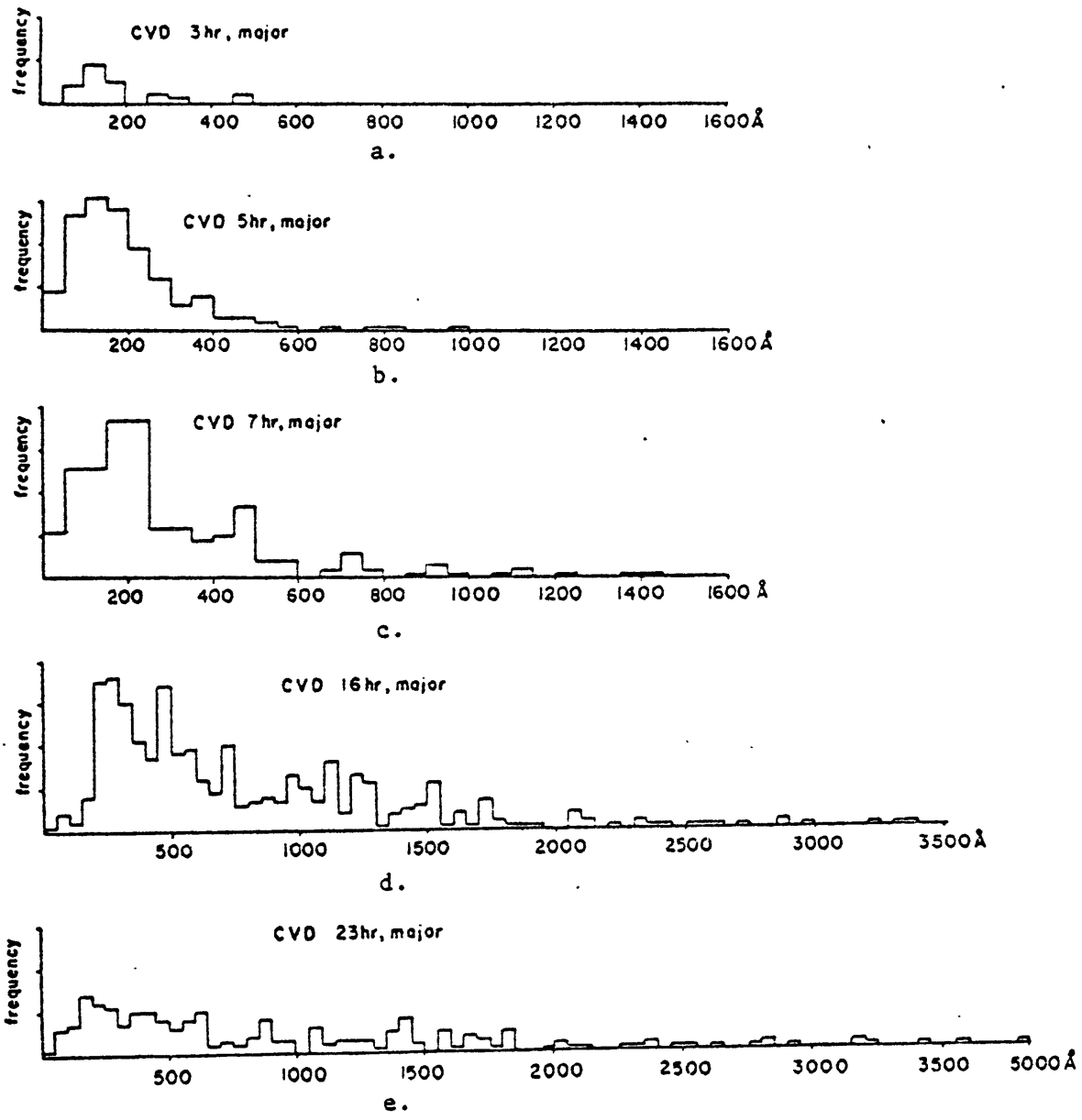

Figure 16: Crystallite size distributions, CVD films at 551°C (Major Axis measured)

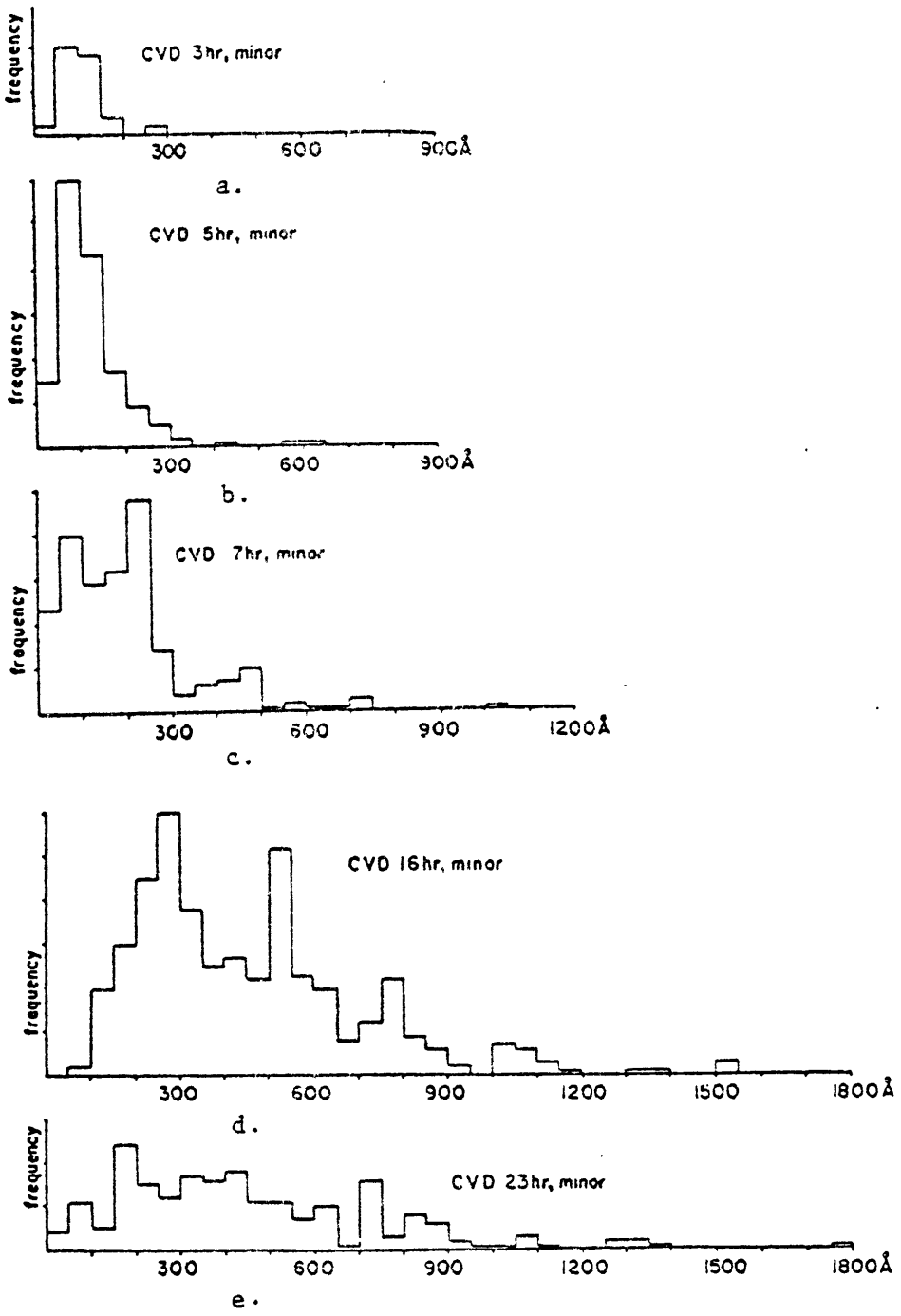

Figure 17: Crystallite size distributions, CVD films at 551°C (Minor axis measured)

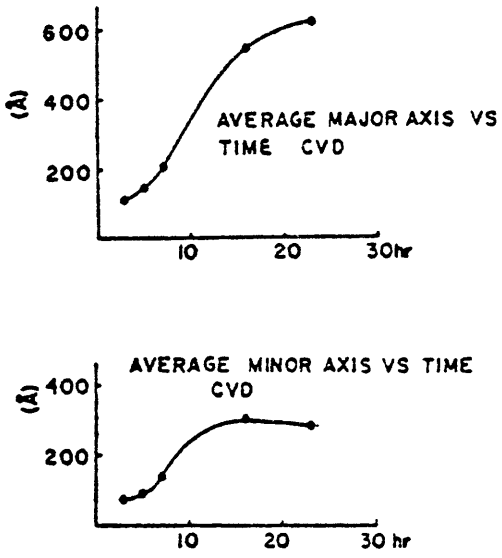

Figure 18: Mean crystallite sizes versus time, CVD films at 551°C

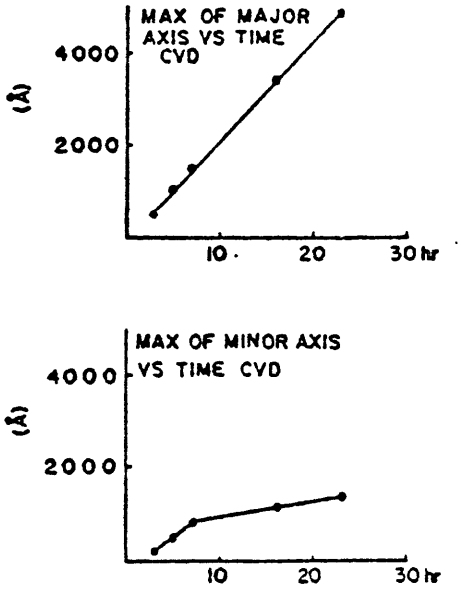

Figure 19: Maximum observed crystallite sizes versus time, CVD films at 551°C

not linear in time, but appears to have an inflection point at 7 hours time (551°C) and is approximately linear for times less than, or greater than this (Figure 19).

This dramatic decrease in the minor axis growth rate calculated from either the mean or maximum observed size suggests that the growth rate along the minor axis decreases with increasing crystallite size. Since the major axis growth rate is constant, the crystallites tend to become elongated as growth proceeds.

The growth rate along the major axis was 6×10^{-3} nm/sec. The growth rate along the minor axis ranges from 4.4×10^{-3} nm/sec to 1.1×10^{-3} nm/sec with increasing time. In contrast, the growth rates reported by Zellama[15] and Koster[14] at 551°C were 1.5×10^{-2} nm/sec and 3.5×10^{-2} nm/sec, respectively.* The growth rate (major axis) for our CVD film** differs from Zellama's growth rate by a factor of about two, and by a factor of about six from Koster's growth rate.

4. Twins

A high density of twins was observed in crystallites grown in a-Si at temperatures between 550 and 725°C. Twins have a characteristic contrast feature in bright-field TEM which consists of parallel (dark) stripes or bands. Crystallites in the CVD films exhibited bundles of twins oriented on or near the major axes, and with other twins branching out of these. Detailed micro-diffraction was not performed

---

* In neither case was the characteristic used to calculate the growth rate specified.

** Our growth rates have not been corrected for the effects of stereographic projection. The correction, on average, will range from a factor of 1 (major/minor axis=1) to 1.6 (major/minor axis=4), hence it tends to increase with increasing crystallite size.

on these crystallites. However, Koster apparently performed that analysis on the lenticular crystallites grown in his evaporated a-Si (T_s=25°C) films.[14] The <211> direction was reported as the fastest growing direction (i.e. the direction along the major axis). Bundles of stacking faults and/or twins were oriented parallel to the fastest growing direction. A strong tendency for twins to branch in other <211> directions was noted.

E. Implications for the fabrication of large grain polycrystalline films

Finally, it is appropriate to comment on the implications of this study to the proposed selective nucleation and growth process for fabricating large grained silicon polycrystalline thin films.

In overview, from this and other works it seems that a relatively high anneal temperature is required to grow a useable large-grained silicon film by this process. Crystallization at relatively low temperatures, 550-724 °C results in heavily twinned grains which have poor electrical characteristics. The ellipsoidal crystallite shapes associated with growth at these temperatures would result in rather high internal grain boundary areas, regardless of grain size. Both of these difficulties can be alleviated by growing crystallites from a-Si at temperatures in excess of 1000 °C.[19,42] Anneal of a-Si at 1000 °C leads to equiaxed, relatively defect free grains in the fully crystallized silicon film.[42] At high anneal temperatures, in excess of 900 °C, the proposed selective nucleation and growth process is facilitated by a decrease in nucleation rate in a-Si with increasing temperature.[14] However, it seems that for a lower temperature process to be viable, growth must be oriented, probably using heteroepitaxy.

VI. Summary and Conclusions

1) Rf-sputtered (T_s=400°C) silicon films have polyhedral coalescense islands with an average diameter of 37.1 nm, as-deposited.

2) Our CVD silicon films had no apparent structure, as-deposited.

3) Both the rf-sputtered and CVD films are amorphous as-deposited, as determined by conventional electron diffraction, and dark-field TEM. However, silicon films which are amorphous by electron diffraction may nonetheless have significant crystallinity by other criteria.

4) Nucleation rates for the rf-sputtered (T_s =400 °C) a-Si film are about two orders of magnitude higher than reported for evaporated (T_s=300°C) a-Si[14] and are over four orders of magnitude higher than reported for evaporated (T_s=25 °C)[15] a-Si, at 724 °C. The steady state nucleation rate for the rf-sputtered film is 4.2×10^{12} /cm^3 s at 724 °C.

5) The rf-sputtered (T_s=400 °C) a-Si film had a transient in nucleation of 1.9 hours at 724 °C which may be related to the high argon content (about 3.6at%) in the film.

6) The growth rates of crystallites in the rf-sputtered films are low, decrease with increasing volume fraction transformed and ultimately stop prior to impingement with adjacent grains. The initial growth rate along the major axis was 6.4×10^{-3} nm/sec at 724 °C. Growth rates of 4.5 to 100 nm/sec have been reported for evaporated a-Si at 724°C.[14-15] No growth in either the maximum size measured, or the mean of the crystallite size distribution is seen for anneals longer than 7.5 hours at 724 °C.

7) Crystallites in the CVD films were shaped like prolate ellipsoids where the deviations from sphericity increase as growth (551-724°C) proceeds. The axial ratios of the crystallites ranged from one (major axis about 5 nm) to four (major axis about 300 nm).

8) The steady state nucleation rate for our CVD film is 1.8×10^{9} /cm^{3} s at 551 °C, which is four orders of magnitude higher than reported for evaporated a-Si at 551°C.[14-15]

9) The transient in nucleation for our CVD film was negligible at 551°C while that reported for evaporated (T_s=25°C) a-Si was 69 hours at 551°C.[14]

10) The growth rate of the major axis of crystallites in our CVD film is 6×10^{-3} nm/sec at 551°C, as compared to reports of 1.5 to 3.5×10^{-3} nm/sec for evaporated a-Si at 551°C.[14-15] The growth rate of the minor axis is initially 4.4×10^{-3} nm/sec and decreases to 1.1×10^{-3} nm/sec for larger crystallites, at 551°C, giving rise to eccentricity in crystallite shape.

VII. Suggestions for further work

1) The nucleation rates, transients and activation energies should be analysed as a function of substrate or reactor chamber temperature during deposition.

2) A more detailed investigation of transient nucleation in the rf-sputtered and CVD films is desirable. This requires detailed nucleation data for anneal times less than 3 hours, at 724 °C for the rf-sputtered film and at 551 °C for the CVD film.

3) An investigation of the effect of dopants on the nucleation rate would significantly contribute to an understanding of nucleation processes in a-Si. Dangling bonds, and their distributions probably have a significant effect on nucleation rates. These, in turn, should be sensitive to doping, particularly by electrically active dopants, such as boron or phosphorus.

4) A comprehensive study which relates the activation energy for growth of the crystallites to their boundary structure is needed for a more quantative understanding of growth processes in the crystallization of a-Si.

5) An investigation of a possible correlation between the deposition temperature and the growth rate during crystallization would be useful, particularly if the primary emphasis was on the relationship of film density to crystallite growth rate.

Appendix 1: Crystallization temperatures for various a-Si films

Silicon film	Anneal temperatures, and times	Crystallinity*
CVD	582-812°C, for 16 hrs	crystalline
	527-551°C, for 16 hrs	amorphous
rf-sputtered		
OS1-022(T_s=23°C)	673°C, for 16 hrs	crystalline
	625-651°C, for 16 hrs	amorphous
	660°C, for 20 hrs	crystalline
	636°C, for 20 hrs	amorphous
	673°C, for 11-16 hrs	crystalline
	660°C, for 20 hrs	crystalline
	660°C, for 18 hrs	amorphous
OS1-023(T_s=400°C)	724-749°C, for 16 hrs	crystalline
	701°C, for 16 hrs	amorphous
	717-724°C, for 20 hrs	crystalline
	686°C, for 20 hrs	amorphous
	717°C, for 20 hrs	crystalline
	717°C, for 18 hrs	amorphous
	724°C, for 16 hrs	crystalline
	724°C, for 15 hrs	amorphous
OS0-024(T_s=400°C)	700-725°C, for 16 hrs	crystalline
OS0-025(T_s=450°C)	625-774°C, for 16 hrs	crystalline

* see Reference 10 for details of the X-ray diffraction technique used in the analysis.

Appendix 2: TEM sample preparation

Sample preparation for transmission electron microscopy (TEM) consisted of five steps:

1) substrate thickness reduced to 0.12 mm by mechanical grinding with 600 mesh SiC slurry
2) 3 mm disks cut out using 600 mesh SiC slurry and a rotating cylindrical brass tool, while the sample is held on a spring loaded jig.
3) Sample is masked for etching. It is mounted on 0.12 mm teflon sheet, which is in contact with the deposited layer. Black wax is applied hot over both the sample and teflon sheet. After the wax solidifies, a 0.6 mm diameter hole is scribed through the wax, in the center of the sample.
4) A hole is etched through the substrate using an etchant employed by Drosd[19] for studies of regrowth of a-Si created by ion-implantation:

   0.125 g Iodine

   55 ml Acetic acid

   28 ml HF

   84 ml HNO_3

During etching, a strong light illuminated the bottom of this sample assembly (step 3). When the sample was etched to within 0.5 μm thickness, light was visible through the sample and it was quickly immersed in deionized water to terminate the etching. Etching rates were about 0.012 mm per minute. The wax was removed with trichloroethylene and the sample rinsed in warm trichloroethylene, acetone and methanol, successively.

5) The sample was ion-milled to perforation from the substrate side. Some milling was then performed on the other surface to remove surface oxides. Typical milling conditions were 10-15 degrees angle, 0.5 mA current per ion gun, 3 kV accelerating potential for a-Si and 4-5 kV for crystalline silicon. The ion-milling rate was about 4 μm/hour per ion gun. The samples were rotated constantly during ion-milling.

Appendix 3: Correlation of density of crystallites apparent in dark-field TEM to the actual density

Since all dark-field work was performed by imaging grains diffracting on (111) planes, the three factors affecting this correlation are: The average number of diffracting planes contributing spots to the (111) diffraction ring per crystallite, the ratio of the total number of grains diffracting on (111) planes to the number being imaged in dark-field, and the ratio of the total number of crystallites to the number oriented such that they diffract on (111) planes. Assessment of these factors involves certain assumptions.

Examination of possible diffraction patterns for diamond cubic structures indicates that, at most, there are four spots corresponding to (111) planes in any of these patterns. An assumption that four spots are contributed to the (111) diffraction ring by each crystallite will result in the most conservative estimate of the nucleation rate. Hence this assumption is used in the calculation of the correlation factor.

The objective aperature of the (TEM) microscope was centered so that it bisected a section of the (111) diffraction ring, thereby subtending 22 degrees of arc-as measured from the transmitted spot. Consequently, only 1 in 16 of the crystallites diffracting on (111) planes is present in the dark-field image if each diffracting crystallite were represented by only one spot on the (111) diffraction ring. Since each diffracting crystallite is represented by four spots on the (111) ring, 1 in 4 crystallites diffracting on (111) planes

appear in the dark-field image. This is strictly true only when the (111) diffraction ring is barely continuous.

Finally, the ratio of the number of crystallites present to those diffracting on (111) planes is needed. In analogy with line broadening in X-ray diffraction, the angle over which the crystal diffracts (about the angles given by Bragg's law)[43] depends on the size of the crystal. Hence the ratio of the number of crystallites present to those diffracting on (111) planes will decrease as the characteristic crystallite size decreases. For the rf-sputtered film the crystallite size is assumed to be 5 nm for the purposes of this calculation. The size of the reciprocal lattice points (diffraction space) corresponding to (111) planes is assumed to be the inverse of the crystallite size.[43] The reciprocal lattice points corresponding to (111) planes have four-fold rotational symmetry. Consider a rotation of the reciprocal lattice, in particular, of the reciprocal lattice points corresponding to (111) planes. Evaluation of the angles over which these (111) planes will diffract relative to the total arc of rotation of a circle leads to an estimate of a 23 to 1 ratio of the total number of crystallites to those diffracting on (111) planes.

Together, these three factors lead to a very conservative estimate for the correlation factor of dark-field to actual crystallite density; this is a factor of 92 to 1.

Bibliography:

1) H. Mahan, SERI private Communication, 1981

2) "Detailed Solar Cell Array Cost", Spectrolab; Division of Textron VII-C-37, 1976

3) L. Kazmerski, Polycrystalline and Amorphous Thin Films and Devices, Academic Press, 1980, ch. 6

4) J.C.C. Fan, "Solar Cells: Plugging into the Sun", Tech. Rev. Aug. 1978, pg. 19

5) H. Ehrenreich and J.H. Martin, "Solar Photovoltaic Energy", Physics Today, Sept. 1979, pg. 26

6) A.K. Ghosh, J. Appl. Phys. 51,(5), 446(1980)

7) J.S. Haggerty and S.C.Danforth, "Controlled Nucleation and Growth Process for large grained Polycrystalline Silicon Photovoltaics", DOE/SERI no. DE-FG02-79ET-00081

8) M. Kinoshita and G. Champier, "Recrystallization of Cast Polycrystalline Silicon", Mat. Sci. &Eng. 47, 29(1981)

9) P.L. Liu, R. Yen, N. Bloembergen and R.T. Hodgson, "Picosecond laser-induced melting and resolidification morphology on Si", Appl. Phys. Lett. 34(12), 864(1979)

10) G. Devaud, "NUCLEATION AND GROWTH BEHAVIOR IN ANNEALED AMORPHOUS SILICON THIN FILMS", B.S. Thesis, Massachusetts Institute of Technology, Dept. of Mat. Sci.&Eng., 1981

11) B.D. King, "CRYSTALLIZATION KINETICS IN ANNEALED AMORPHOUS SILICON THIN FILMS", B.S. Thesis, Massachusetts Institute of Technology, Dept. of Mat. Sci.&Eng., 1981

12) N.J. Shevchick and W. Paul, "Voids in Amorphous Semiconductors", J. Non-Cryst. Sol. 16, 55(1974)

13) D. Turnbull and J.C. Fisher, J. Chem. Phys. 17, 71(1949)

14) U. Koster, "Crystallization of Amorphous Silicon Films", Phys. Stat. Sol.(a) 48, 313(1978)

15) K. Zellama, P. Germain, S. Squelard, J.C. Bourgoin and P.A. Thomas, "Crystallization in Amorphous Silicon", J. Appl. Phys. 50(11), 6995(1979)

16) D. Kashchiev, "Solution of the non-steady state problem in Nucleation Kinetics", Surf. Sci. 14, 209(1969)

17) W.A. Harrison, Surf. Sci. 55, 1(1976)

18) F. Spaepen, "A structural model for the interface between amorphous and crystalline Si or Ge", Acta. Met. 26, 1167(1978)

19) R.M. Drosd,"A Model of the Recrystallization Mechanism of Amorphous Silicon layers created by Ion-Implantation", Ph.D. Thesis, Lawrence Livermore Laboratory, Univ. of California, 1980

R.M. Drosd and J. Washburn, "A new technique for observing the amorphous to crystalline transformation in thin surface layers on silicon wafers", J. Appl. Phys. 51(8), 4106(1980)

20) L. Csegregi, E.F. Kennedy, J.W. Mayer and T.W. Sigmon, "Substrate-orientation dependence of the epitaxial regrowth rate from Si-implanted amorphous Si", J. Appl. Phys. 49(7), 3906(1978)

21) E.F. Kennedy, L Csepregi, J.W. Mayer and T.W. Sigmon, "Influence of ^{16}O, ^{12}C, ^{14}N and noble gases on the crystallization of amorphous Si", J. Appl. Phys. 48(10), 4241(1977)

22) L. Csepregi, E.F. Kennedy, T.J. Gallagher, J.W. Mayer and T.W. Sigmon, "Reordering of amorphous layers of Si implanted with ^{31}P, ^{75}As, ^{11}B ions", J. Appl. Phys. 48(10), 4234(1977)

23) D.R. Hamilton and R.G. Seidensticker, "Propagation Mechanism of Germanium Dendrites", 31(7), 1165(1960)

24) J.C. Bean and J.M. Poate, "Evidence for void interconnection in evaporated amorphous silicon from epitaxial crystallization measurements", Appl. Phys. Lett. 36(1), 61(1980)

25) D. Turnbull, "Theory of Grain Boundary Migration Rates", Trans. AIME 191, 661(1951)

26) G. Shimaoka and S.C. Chang, "Structure of Silicon Films Evaporated onto a NaCl substrate", J. Vac. Sci. Technol. 9(1), 235(1972)

27) M. Janai, D.D. Allred, D.C. Booth and B.O. Seraphin,"Optical properties and structure of amorphous silicon films prepared by CVD", Solar Energy Mats. 1, 11(1979)

28) D. Adler, M.I.T., Private Communication, 1981

29) P.D. Davidse and L.I. Maissel, "Dielectric Thin Films through rf-sputtering", J. Appl. Phys. 37(2), 574(1966)

30) J. Vander Sande, M.I.T., Private Communication, 1981

31) D.E. Polk, "Structural Model for Amorphous Silicon and Germanium", J. Non-Cryst. Sol. 5, 365(1971)

32) M.L. Rudee and A. Howie, "The Structure of Amorphous Si and Ge", Phil. Mag. 25(4), 1001(1972)

33) F. Spaepen and R.M. Meyer, "Optical Modeling of Electron Microscopy on Amorphous Tetrahedrally Coordinated Materials", J. Non-Cryst. Sol. 13, 440(1973/1974)

34) A. Howie, "High Resolution Electron Microscopy of Amorphous Thin Films", J. Non-Cryst. Sol. 31, 41(1978)

35) J.C. Knights, R.A. Lujan, M.P. Rosenblum, R.A. Street, D.K. Bieglesen and J.A. Reimer, "Effects of inert gas dilution on plasma-deposited a-Si:H films", Appl. Phys. Lett. 38(5), 331(1981)

J.C. Knights, "Characterization of Plasma-Deposited Amorphous Si:H thin films", Proceedings of the 10th Conference on Solid State Devices, Tokyo 1978; Jap. J. of Appl. Phys. 18, Suppliment 18-1, 101(1979)

J.A. Reimer, R.W. Vaughan and J.C. Knights, "Proton NMR studies of annealed plasma-deposited amorphous Si:H films", Sol. State Comm. 37, 161(1981)

A.J. Leadbetter, A.A.M. Rashid, R.M. Richardson, A.F. Wright and J.C. Knights, "Small angle x-ray and neutron scattering studies of plasma-deposited amorphous silicon-hydrogen films", Sol. State Comm. 33, 973(1980)

36) L. Maissel and R. Glang, Handbook of Thin Film Technology, Mc-Graw Hill, N.Y. 1970, Ch. 8

37) S.C. Moss and J.R. Graczyk in Proc. 10th Int. Conf. on the Physics of Semiconductors, (eds. S.P. Keller, J.C. Hensel and F. Stern), Cambridge MA 1970, U.S. Atomic Energy Commission, Washington 1970, pg. 658

38) P. Revesz, M. Wittmer, J. Roth and J.W. Mayer, "Epitaxial regrowth of Ar-implanted amorphous silicon", J. Appl. Phys. 49(10), 5199(1978)

39) W.T. Pawlewicz, "Influence of Deposition Conditions on Sputter-Deposited Amorphous Silicon", J. Appl. Phys. 49(11), 5595(1978)

R. Messier, T. Takamori and R. Roy, "Structure-composition variation in rf-sputtered films of Ge caused by process parameter changes", J. Vac. Sci. Technol. 13(5), 1060(1976)

40) W.D. Kingery, H.K. Bowen and D.R. Uhlmann, Introduction to Ceramics, Wiley, 1976 pg. 457

41) R.A. Swalin, Thermodynamics of Solids, Wiley, 1972, pg. 182

KINETICS OF CRYSTALLIZATION OF SELECTED AMORPHOUS SILICON FILMS

by

FRANKLIN DAVID VAN GIESON

Submitted to the Department of Materials Science and Engineering
on May 7, 1982 in partial fulfillment of the requirements for
the Degree of Master of Science in
Ceramics

ABSTRACT

Nucleation and growth rates in the crystallization of amorphous silicon (a-Si) films deposited by rf-sputtering and CVD were measured by TEM. Both types of films were determined to be amorphous as-deposited by electron diffraction. Unlike the CVD film, the rf-sputtered film had internal structure as-deposited, namely coalescense islands. These islands, and argon trapped in the rf-sputtered film slowed or arrested the growth of crystalline silicon. The growth of crystallites in the CVD film was anisotropic and somewhat slower than reported for evaporated a-Si films, at 551°C. Nucleation rates in both the rf-sputtered films at 724°C and the CVD films at 551°C were about four orders of magnitude higher than in some evaporated a-Si films at these temperatures.

Thesis Supervisor: Dr. John S. Haggerty
Title: Senior Research Scientist

Co-Thesis Supervisor: Dr. Kenneth C. Russell
Title: Professor of Metallurgy

I. INTRODUCTION

This research program is directed toward development of a controlled crystallization process for large grained polycrystalline thin film Si for photovoltaic applications. The impetus for this work is to reduce the cost of PV devices. This can be done either by attempting to develop new, cheaper methods of crystal growth, or developing a different technology altogether.

Single crystal Si devices in PV applications exhibit high efficiencies and durability.[1] Despite this promise, we feel that these processes may always be expensive relative to the cost targets for photovoltaics because of the low growth rates associated with single crystal growth processes.

An alternate technology currently under investigation involves use of amorphous (a)-semiconductors such as hydrogenated Si or chalcogenide glasses[2] as the active material. Although these materials can be processed using high deposition rates and thin film processes, and hence have very low potential costs, their efficiencies have been low (6-7%[3] for a-Si-H) and they have unresolved durability issues. It is not clear yet that their efficiencies can be raised to levels above 10%, which are necessary before solar a-Si-H cells will be competitive with other means of power generation.[4]

Still another alternative, which we have dealt with in this research program, is to use polycrystalline silicon (and other

materials) as the basis for thin film photovoltaics. Polycrystalline silicon thin film devices potentially have numerous advantages over both single crystal and amorphous thin film devices; namely the high efficiency and high durability of single crystal Si, and thin film techniques associated with a-Si technology. The process we have investigated would combine these attributes.

This process is one of controlled transformation from a-Si to large grained polycrystalline silicon from precisely located nuclei. These crystalline nuclei could be grown to a size limited solely by impingement of simultaneously growing grains, while suppressing homogeneous nucleation in the still amorphous film. While the process has some characteristics of grain growth, it is, in fact, a controlled transformation process as used in glass ceramics (Pyroceram™).

The first step is to deposit amorphous Si films onto a suitable substrate. The thin films will then be inoculated (seeded) with crystalline nuclei in a controlled manner at specific locations by localized heating using a laser or other appropriate means (heated stylus etc.). The crystalline nuclei would be placed in a grid pattern with a spacing on the order of 1 cm. These nuclei would then grow during an isothermal anneal, under conditions optimized to achieve acceptably high growth (transformation) rates while maintaining the spontaneous nucleation rate at zero. If sucessful, the result would be a polycrystalline thin film Si device whose grain size is determined by the original seed spacing i.e. ≈ 1 cm.

It has been demonstrated that the grain size of a polycrystalline thin film photovoltaic device must be >> the film thickness to achieve nearly single crystal efficiencies (10-15%).[5] Achievement of large grain size to film thickness ratios by conventional annealing of fine grained polycrystalline films has not been possible due to the nature of the driving force and interactions between the grain boundaries and the films surface.

For the process of controlled nucleation and growth, the driving force for the growth of inoculated crystalline grains is the change in free energy on transformation from amorphous to crystalline silicon minus a small term corresponding to the increase in boundary surface energy. The driving force for crystallization is much larger than that for conventional grain growth and continues to force the growth of the crystalline phase effectively independent of grain size. This boundary can have a much higher mobility than a conventional grain boundary. Growth rates from epitaxial regrowth experiments of ion-implanted a-Si,[6] and UHV E-beam evaporated Si films[7] indicate (Figure 1) that at 700°C, the time needed to grow a 1 mm radius grain would be on the order of 500 minutes; while at 800°C the time needed would be only 50 minutes. Annealing of laser inoculated a-Si films with these high growth rates, should result in the desired large grained polycrystalline thin film Si, provided that spontaneous nucleation can be supressed.

There are several key issues that we have considered critical for this process to be practical. The most important issue is the ability

to separate the phenomena of nucleation from that of growth of crystalline Si into the a-Si film. We must be able to isothermally anneal the films to cause the inoculated crystallites to grow without spontaneous nucleation of crystalline Si in the as yet untransformed regions of the film, i.e. there must be a temperature window where the growth rates for the inoculated crystallites are high, $> 10^4$ Å/min, yet the spontaneous nucleation rates are $\simeq$ zero.

The choice of a deposition technique is also critical. The deposition method and the specific process variables, i.e. pressure, gases used, substrate temperature, and deposition rate etc, will determine the atomic structure, microstructure, density, and purity of the deposited films. These film characteristics control the nucleation and growth rates of the crystalline Si in the a-Si films. We have surveyed different deposition processes to evaluate their prospects for generation of large grained polycrystalline thin films.

Suitable substrate materials must be chemically, and thermo-mechanically compatible with both the a-Si and crystalline Si over the entire temperature range experienced during processing. They should also have a smooth dense surface to avoid both spurious nucleation and interferance with growth. Amorphous substrates are preferred to avoid any epitaxial interactions between the substrate and film. After a brief effort to evaluate substrates, we bypassed this issue and selected one that we knew would be suitable for process demonstration purposes.

The optical characteristics of the Si film, thermal conductivity of the substrate, choice of laser wavelength, etc. will combine to determine the ability to successfully inoculate crystalline embryos in the a-Si films. Due to the extensive work on laser recrystallization in the literature, laser inoculation was not considered to present a major problem.

II. EXPERIMENTAL

A. Substrates

Three materials were chosen for investigation as substrates: fused silica, vitreous carbon*, and oxidized** single crystal Si wafers. The thermal expansion mismatch with SiO_2 caused the Si films to crack and there were severe adhesion problems with the vitreous carbon substrates. Only oxidized silicon wafers were found to be suitable for process demonstration experiments.

B. Film Deposition

Amorphous Si films have been deposited using RF sputtering, E-beam evaporation, and a CVD reactor. Prior to deposition, substrates were cleaned and degreased. RF sputtering, on an MRC 8620, was performed using a water cooled high purity polycrystalline Si target and argon

* Gallard Schlesinger
** Mosfet Microlabs

gas (sample target spacing = 5.5 cm). The chamber was evacuated to 3 x 10^{-6} torr prior to plasma ignition at 7-9 millitorr. The resulting deposition rates with 200 watts power were ~1 μm/hr (167 Å/min) with typical film thicknesses of 1-2 μm. The major deposition process variable examined was the effect of substrate temperature (RT to 450°C) on the film's spontaneous crystallization behavior.

Electron beam evaporation was performed in a Sloan evaporator, using a high purity polycrystalline Si target in a vitreous carbon hearth liner. The pre-deposition pressure was 1 x 10^{-7} torr. During evaporation at a rate of 100 Å/sec, the pressure was 5 x 10^{-6} torr. Substrates were water cooled and film thicknesses were 7,500 Å.

A third set of a-Si films was prepared at M.I.T. Lincoln Laboratories* using a General Signal Communications CVD reactor. The reaction proceeded with a substrate temperature of 610°C using 90 cc/min of 5% SiH_4-argon and 90 cc/min of N_2 following the reaction $SiH_4 \rightarrow Si+2H_2$. The deposition rate was 200 Å/min and the films were 1 μm thick.

C. Spontaneous Crystallization

Isothermal annealing experiments were performed in a Vycor™ muffle furnace using flowing high purity He to determine the spontaneous crystallization behavior of the various films studied, i.e. evaluate the nucleation and growth rates for the films. It was presumed that the growth rates from work cited in the literature could be used until

* Professor H. Smith and Dr. M. Geiss

values were available from our own results. The spontaneous crystallization behavior allowed us to empirically screen the deposition processes and process variables.

D. Laser Inoculation

A CO_2* laser and Nd:YAG** laser were used for the initial laser inoculation work. The low optical absorptivity of Si at the wavelength of the CO_2 laser and poor stability and torroidal shape of the Nd:YAG laser beam lead to the use of an argon laser. Laser inoculation experiments have been performed in an inert atmosphere primarily with an 8 watt CW argon ion laser† operating at λ = 0.48 μm with a 1.23 cm focal length lense. Power levels ranged from 0.3 to 2.0 watts and shutter speeds from 1 m sec to 1 sec.

E. Film Characterization

The following methods were used to characterize the films: interference and infrared microscopy, SEM (with grain boundary etching), TEM (electron diffraction, bright field and dark field imaging), and X-ray diffraction. A X-ray technique has been developed which involves a glancing angle Debye-Scherrer method using a single crystal goniometer and a Weissenberg camera to achieve increased

* Coherent 150 (λ = 10.591 μm)
** Quanta Ray (λ = 0.532 μm)
† Spectra Physics 171

diffraction volume. X-ray fluorescence and SIMS* were used to measure the impurities present in the Si films.

III. RESUSTS AND DISCUSSION

In general terms, the results showed that the deposition technique and process parameters had strong influences on the crystallization behavior. Within the range of process variables examined, we were able to produce films which exhibited spontaneous crystallization times and temperatures which should have permited large grain sizes to be achieved using the process outlined.

The RF sputtered films were all amorphous to X-ray diffraction for substrate temperatures up to 450°C. Isothermal anneals performed to evaluate the spontaneous crystallization temperature revealed a strong dependance on the substrate temperature during deposition. Films deposited at 23, 300, 400, and 450°C substrate temperatures crystallized at 630°C, 690°C, 725°C, and < 675°C respectively for 16 hour anneals. Increasing the substrate temperature raised the crystallization temperature by ~ 100°C, to the temperature range where one would expect the desired high growth rates (> 10^4 Å/min).

For room temperature substrates, films annealed at 673°C had a time to crystallize between 7 and 10 hours while at 600°C the time was 12 to 16 hours (Figure 2). For the 400°C substrate temperature films, the incubation period was 15 to 16 hours at 725°C and 18 to 20 hours at

* Charles Evans and Associates, San Mateo, CA.

717°C. This longer time to crystallize is likely related to the higher crystallization temperature for the heated substrate films.

The E-beam films had a 16 hour crystallization temperature between 600 and 700°C while Blum[11] found 605°C for E-beam films. The CVD films crystallized at the lowest temperature of all films, between 551 and 581°C.

For the RF sputtered films, it can be seen that for both RT and 400°C substrate temperatures, the time to crystallize (as determined by X-ray) is longer than that observed by Blum[11] for E-beam deposited films. We now know that some annealed films determined to be amorphous by X-ray are partially crystalline (TEM), i.e. the sensitivity of the X-ray technique to the onset of crystallization is poor. This may explain part of the observed behavior. We do feel however, that the differences observed between the crystallization behavior of our films, and the fact that the time to crystallize plots have the same slope as Blum's[11] (320 KJ/mole) are both significant.

At this point in time, with only the X-ray results at hand, we attempted to seed the a-Si films with crystalline nuclei. Using the oxidized single crystal substrates and 1.2 μm thick RF sputtered films (T_{sub}= 400°C), we were able to seed the films with crystallites under the following conditions: He atmosphere, 100 msec shutter, 2.0 watts CW, and a spot size of 20 or 57 μm, (6.4×10^4 and 7.8×10^3 J/cm^2). For the 20 μm spot size, the crystalline seeds extended some 10 to 20 μm beyond the central laser spot indicating either rapid growth at elevated temperatures or crystallization from a melt. At the beam

center, the film was partially ablated. For laser spot sizes > 167 μm (9.13×10^2 J/cm^2) no crystalline seeds were observed. Grain growth anneals were conducted in flowing He at 700°C for 10 hours. Based on the epitaxial regrowth rates of ion implanted and UHV E-beam Si, (Figure 1) we anticipated that the laser inoculated crystallites would grow at a rate of 1 μm/min to a final size of 600 μm. Instead growth rates were approximately 1 Å/min.

Despite evidence of crystalline seeds in the laser inoculated RF sputtered T_{sub} = 400°C films, it is clear that the seeded films did not show the high growth rates associated with high purity films. This result dictated a shift in our efforts toward an investigation of the spontaneous crystallization behavior of the films and the factors causing the low observed growth rates. The detailed results of this TEM study are presented in Appendix I "Kinetics of Crystallization of Selected Amorphous Silicon Films", M.S. Thesis by F. Van Gieson.

None of the as-deposited RF sputtered films revealed any discernable structure which could be interpreted as crystallinity. The 400°C substrate temperature films were found to contain a 370 Å cellular type structure similar to the "poly-amorphous" boundaries observed in hydrogenated a-Si films by Knights.[12] This structure may be attributable to columnar type growth of the films. Dark field TEM of films annealed for 3.5 hours at 724°C revealed only a few isolated crystallites approximately 150 Å in size. As the transformation proceeds, nucleation continues, and the density of crystallites increases to the point where the film is crystalline by X-ray

diffraction (16 hours). Throughout the transformation process, there appears to be an upper limit to the crystallite size of approximately 350-400 Å. This striking feature suggests that some microstructural feature such as the internal boundaries appears to be limiting grain growth.

The measured nucleation rate for these RF sputtered films is $4 \times 10^{12}/cm^3$-sec at 724°C, which is between two and four orders of magnitude higher than for Zellama's[13] or Koster's[14] E-beam evaporated films. The growth rate for the RF sputtered Si is ≈ 4 Å/min at 724°C, nearly three orders of magnitude slower then values reported by Zellama[13] or Koster[14]. With more precise observations, it is apparent that the nucleation and growth characteristics of the RF sputtered a-Si films are not appropriate for the controlled transformation process under investigation.

The as-deposited CVD films were amorphous and featureless as seen in TEM. Examination of the early stages of spontaneous crystallization (5 hrs at 551°C) revealed isolated crystallites (300 to 1000 Å in size) with somewhat elongated morphologies. At later stages, (23 hrs) there was a higher nuclei density. In addition, grain growth continued throughout the annealing process to the point of impingement with other simultaneously growing grains, in contrast to the RF sputtered case. The fully transformed CVD crystallites appeared ellipsoidal in shape with an aspect ratio on the order of 3:1 with a major axis length of from 1000 to 4000 Å.

These CVD films have nucleation rates of $\approx 2 \times 10^9/cm^3$-sec at 551°C which is four orders of magnitude higher than those reported by Zellama[13] and Koster[14]. In contrast to this, the growth rates for the CVD films are only a factor of 2-4 below that for Zellama's[13] and Koster's[14] E-beam films. It should be noted that this is only a factor of 20 below that reported for the epitaxial regrowth rates shown in Figure 1.

TEM characterization of the as-deposited E-beam samples shows virtually no structural details. The films yielded amorphous diffraction patterns. We have not yet examined the crystallized E-beam samples by TEM.

Chemical analysis revealed that none of the films were as pure as we had anticipated nor as pure as is needed to achieve the high growth rates desired.

X-ray flourescence analysis showed that the RF sputtered films contained ≈ 2 wt % argon. Films sputtered at lower deposition rates contained less argon. In any case, the bulk of the argon remained in the films after crystallization.

SIMS analysis of the various films is summarized in Table I. It should be noted that Evans and Associates indicated a lack of confidence in the argon count rates as they had not done that analysis before.

It is clear that the RF sputtered films had significant levels of O, C, and H, (some of the O and C may come from atmospheric contamination of the porous films). The E-beam films had significant

levels of H, O, and C. While the O may have come from atmospheric contamination, the high C content probably resulted from the use of a C hearth liner during evaporation. The CVD films also had significant levels of O, C, and H_2 where the high H content probably resulted from the excess H present from the decomposition of SiH_4.

In the case of the RF sputtered films, it is clear that the as deposited films have an internal boundary type structure. Many a-Si films have also been reported to have densities ranging to 15% less than that of crystalline Si[15] as a result of an internal network of micro-voids[16-19] approximately of 50 Å in size. We estimate a density 10% lower than the crystalline value for our RF sputtered films based on a volume change on crystallization. It is possible that either the void surfaces or the poly-amorphous boundaries may be acting as heterogeneous nucleation sites and barriers to growth; thereby largely controlling the nucleation rates and the final crystallite size. In addition the high levels of impurities, especially argon, will have a significant detremental effect on the growth rates as seen in Figure 1.

The CVD films have no obvious internal microstructure that is controlling the nucleation behavior. It is likely that the high substrate temperature during deposition results in a significant number of critical sized crystalline nuclei in the as-deposited films which, although not observable in TEM, are controlling the nucleation rate yielding such extremely high values.

The growth of crystallites in the CVD films was quite well behaved. The only impediment to growth was impingement of simultaneously growing grains, the resultant grain size being effectively determined by the high nucleation rate. Despite the relatively high concentration of impurities, the observed growth rate (extrapolated to $\approx 10^4$ A/min at 850°C) is fairly close to that predicted by the epitaxial regrowth studies. This is close to the range required for sucessful process demonstration.

IV. SUMMARY

Based on the work of this project it appears that our concept of a process to generate large grained polycrystalline thin films is still valid; i.e. deposit an amorphous film, inoculate it with crystallites at specific locations, and then induce growth during an isothermal anneal. The most important issue is still the ability to separate the nucleation process from that of growth. It is evident that the ability to make this seperation depends on the characteristics of the deposition process primarily through the resultant structure and purity of the deposited films.

Clearly, inert gas plasma deposition techniques results in films that have internal structures, and/or significant levels of impurities which result in inherently high nucleation rates and/or low growth rates. These deposition processes do not appear suitable for this application.

There is clear evidence in the literature[6,7] for solid state epitaxial regrowth with the desired high growth rates in both ion implanted and UHV E-beam deposited layers in the temperature range of 500-875°C. Also, growth proceeded for long distances without the occurance of spontaneous nucleation ahead of the transformation boundary. The CVD films examined have exhibited growth rates near those necessary for successful process demonstration, yet the nucleation rates are prohibitavely high.

It remains to be seen whether conventional CVD or E-beam deposition techniques can produce films with suitable characteristics without excessively high costs. We are currently developing a novel laser driven CVD process that has some promise for yielding a-Si films with the crystallization behavior necessary for this process of controlled nucleation and growth. With this new process, substrate temperatures are maintained at much lower levels than conventional CVD processes. However it is done, a deposition process must be defined that results in films with low nucleation rates (i.e. low substrate deposition temperatures), but also generate films with impurity levels of approximately 10^{18}-$10^{19}/cm^3$.

V. REFERENCES

1. J.C.C. Fan Techn. Rev. 18-36 Aug-Sept (78)

2. D. Adler, private communication.

3. D.E. Carlson, C.R. Wronski, J.I. Pankove, P.J. Zanaucchi and D.L. Staebler, RCA Review (1977).

4. T.L. Chu, S.S. Chu, E.S. Stokes, C.C. Lin, R. Abdernassoul "Thin Film Polycrystalline Si Solar Cells", 13th IEEE

5. A. Ghosh, C. Fishman, T. Feng. "Theory of the Electrical and Photovoltaic Properties of Polycrystalline Si", J. Appl. Phys., 51, 446 - 54, (1980).

6. T.O. Sedgewick, "A Simple Optical Pyrometer for In Situ Temperature Measurement During CW Argon Laser Annealing", Laser and Electron-Beam Solid Interactions and Materials Processing, 147 - 153, 1981 Eds. Gibbons, Sigmon, Hess.

7. J.A. Roth, G.L. Olson, S.A. Kokorowski, L.D. Hess "Laser Induced Solid Phase Epitaxy of Silicon Deposited Films", Laser and Electron-Beam Solid Interactions and Materials Processing, 413, 1981 Eds. Gibbons, Sigmon, Hess.

8. R.M. Drosd and J. Washburn, "A New Technique for Observing the Amorphous to Crystalline Transformation in Thin Surface Layers on Silicon Wafers", J. Appl. Phys. 51 (8), 4106 (1980).

9. L. Csepregi, E.F. Kennedy, T.J. Gallagher, J.W. Mayer and T.W. Sigmon, "Reordering of Amorphous Layers of Si Implanted with ^{31}P, ^{75}As, ^{11}B Ions", J. Appl. Phys. 48 (10), 4234 (1977).

10. E.F. Kennedy, L. Csepregi, J.W. Mayer and T.W. Sigmon, "Influence of ^{16}O, ^{12}C, ^{14}N and Noble Gases on the Crystallization of Amorphous Si", J. Appl. Phys. 48 (10), 4241 (1977),

11. N. Blum, C. Feldman "Crystallization of Amorphous Silicon Films", Phys. Stat. Sol., (a) 48, 313, (1978).

12. J.C. Knights, "Characterization of Plasma-Deposited Amorphous Si:H Thin Films", Proceedings of the 10th Conference on Solid State Devices, Tokyo 1978; Jap. J. of Appl. Phys. 18, Suppl. 18-1, 101 (1979).

13. K. Zellema, P. Germain, S. Squelard, J.S. Bourgoin and P.A. Thomas, "Crystallization in Amorphous Silicon Films", J. Appl. Phys., 50 (11) 6995 (1979).

14. U. Koster "Crystallization of Amorphous Silicon Films", Phys. Stat. Sol. 48, 313 - 21 (1978).

15. S.C. Moss, J.F. Graczyk Phys. Rev. Lett. 23, 1167 (1969).

16. M.L. Theye, A. Gheorghio, M. Gandais, S. Fisson, "Structural Relaxation and Crystallization of Amorphous Ge Films", J. Non Cryst Sol. 37, 301-23, (1980).

17. W.T. Pawlewicz, "Influence of Depositions Conditions on Sputter-Deposited Amorphous Silicon" J. Appl. Phys., 49, (11), (1978).

18. T. Shinizu, M. Kumeda, I. Watanabe, Y. Kiriyama, Jap. J. Appl. Phys., 19, No. 5, L235-8, (1980).

19. H. Frtizsche, C.C. Tsai Solar Energy Materials 1, 471-9, (1979).

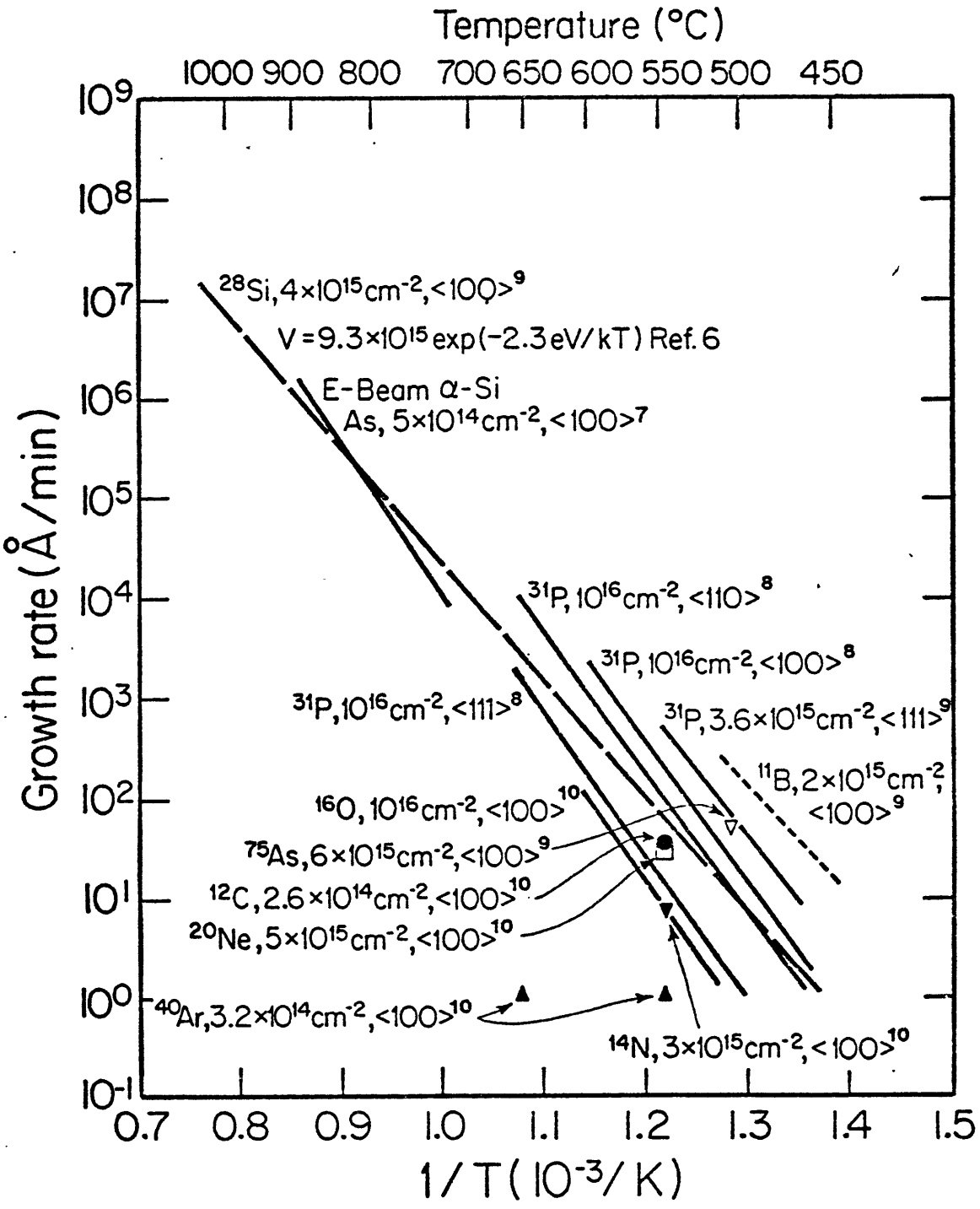

Figure 1. Epitaxial Regrowth Rates for Ion Implanted and E-Beam Deposited a-Films.

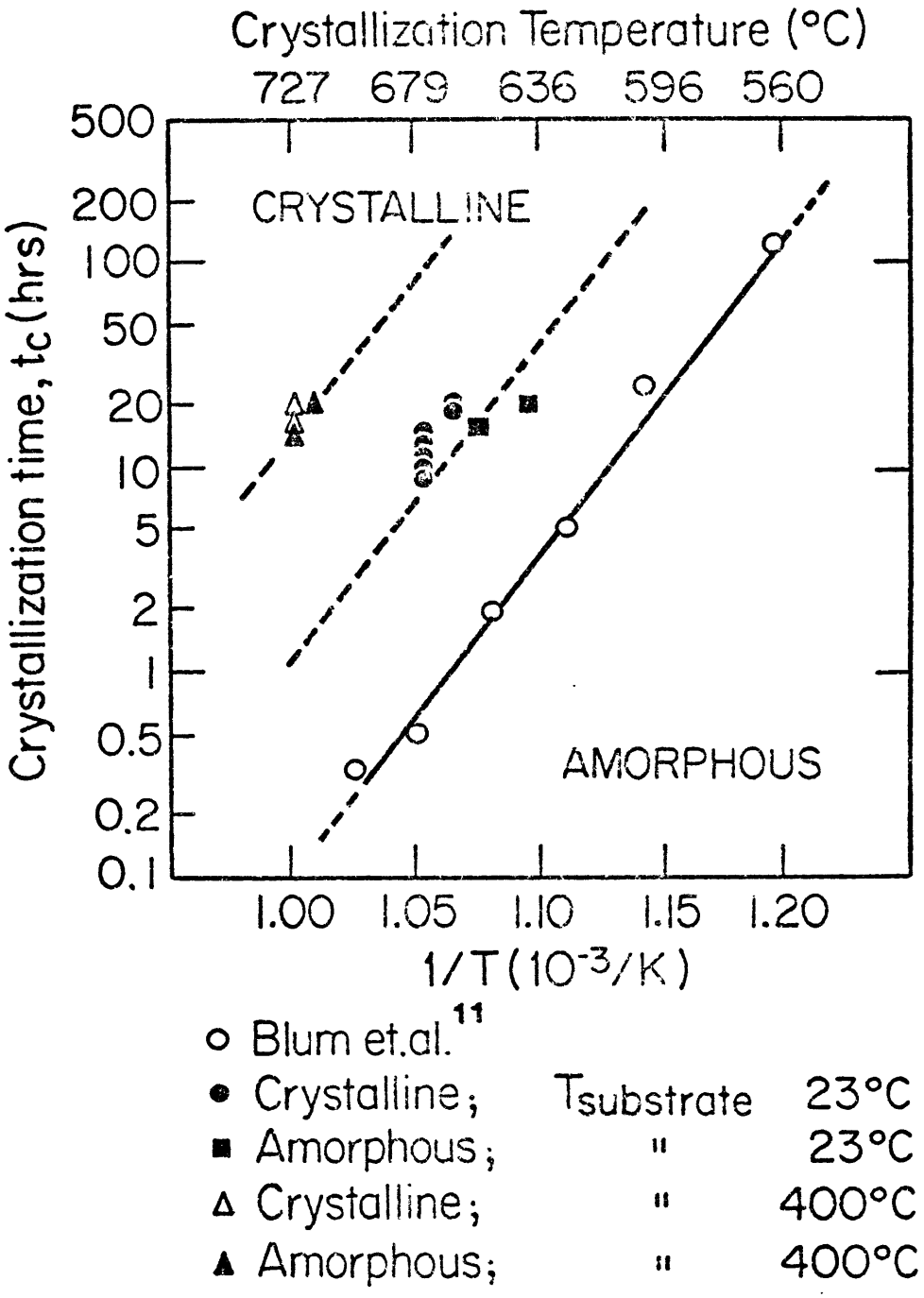

Figure 2. Crystallization Times for RF Sputtered a-Si Films.

TABLE I

Ion	RF Sputtered T_{sub} 400°C	E-beam T_{sub} 23°C	CVD T_{sub} 610°C	Czochralski Crystal
^{14}Si	4×10^5 cts/sec	5×10^5 cts/sec	5×10^5 cts/sec	5×10^5 cts/sec
^{11}B	50 cts/sec	7×10^2 cts/sec	1×10^2 cts/sec	30 cts/sec
^{38}Ar	3×10^2 cts/sec	1×10^2 cts/sec	3×10^2 cts/sec	50 cts/sec
^{16}O	2×10^{20} atoms/cm^3	2×10^{21} atoms/cm^3	3×10^{20} atoms/cm^3	1×10^{18} atoms/cm^3
^{12}C	6×10^{20} atoms/cm^3	3×10^{21} atoms/cm^3	2×10^{19} atoms/cm^3	10^{18} to 10^{20} atoms/cm^3
^{1}H	1×10^{20} atoms/cm^3	7×10^{19} atoms/cm^3	2×10^{20} atoms/cm^3	1×10^{19} atoms/cm^3